SEPARATION OF OIL FROM OIL WATER EMULSION BY THE USE OF ALGINATE GEL ENCAPSULATED IRON OXIDE AND GRAPHENE OXIDE NANOPARTICLES

By

Nikhil Ket, B.E.

A Thesis Submitted in Partial Fulfillment of the Requirements

for the Degree of

Master of Science

in

Petro – Environmental Science: Interdisciplinary Program

University of Alaska Fairbanks

May 2017

APPROVED:

Dr. Srijan Aggarwal, Committee Chair
Dr. Shirish Patil, Committee Co-Chair
Dr. Lei Zhang, Committee Member
Dr. Leroy Hulsey, Chair
Department of Civil and Environmental Engineering
Dr. Douglas J. Goering, Dean
College of Engineering and Mines
Dr. Michael Castellini, *Dean of the Graduate School*

Abstract

Crude oil is used extensively around the world as a source of energy and as a means of producing various petroleum products. However, apart from being an excellent energy source, crude oil can also be a major pollutant in the form of oil spills. Crude oil spills can occur on land and in the ocean during the drilling, production, transportation or storage stages. While it is possible to reduce the damage caused to the environment by an oil spill, it is almost impossible to completely remove the adverse effects. New techniques need to be developed to clean-up oil spills at higher rates and with increased efficiency.

The use of nanoparticles (NPs) for oil spill clean-up has gained popularity in recent years. This research focuses on the use of alginate gel as an immobilizing agent for nanoparticles that are then used for the removal of heating oil from an oil-water mixture. Iron Oxide and Graphene Oxide Nanoparticles were immobilized using sodium alginate in calcium chloride. The concentration of the nanoparticles was varied from 1 g/L to 5 g/L. The immobilized nanoparticles were then added to an oil-water mixture which was prepared by spiking heating oil in methanol and adding the solution to deionized water to achieve uniform distribution. 10 mL samples containing residual oil were extracted from the heating oil and water mixture at regular intervals and were analyzed for the residual oil. Measurements were carried out for residual hydrocarbons using Gas Chromatography/Mass Spectroscopy (GC/MS), Fluorescence Spectroscopy and Ultraviolet–visible spectroscopy (UV-Vis). Results from GC/MS show the highest percentage of oil being removed from the mixture by 2 g/L iron oxide (77%) and 2 g/L graphene oxide (81%) NPs. Analysis for residual hydrocarbons based on the time of contact showed promising results, with 75% of oil removed in 70 minutes. Further, based on the data obtained it was observed that the nanoparticles reached saturation after 70 minutes and were unable to remove additional quantities

of oil from the mixture. Changing the nanoparticles from Iron Oxide to Graphene Oxide increased the amount of oil removed by 4%. This research will assist future development of oil spill clean-up and water treatment techniques that make use of nanoparticles as sorbents.

Table of Contents

Page

List of Figures

Page

List of Tables

Page

Acknowledgements

First of all, I would like to extend my gratitude to the chair of my advisory committee, Dr. Srijan Aggarwal, for his invaluable guidance, encouragement, and constant support during the entirety of this project. It gives me great pleasure to show my appreciation to my committee members, Dr. Shirish Patil and Dr. Lei Zhang for their valuable suggestions during this work. I have learned a lot from them.

I wish to thank Dr. Shirish Patil for his time spent with me as the member for this project. Dr. Patil was able to provide valuable assistance when needed from King Fahd University of Petroleum and Minerals (KFUPM) in Saudi Arabia, where he is now Saudi Aramco Chair Professor of Petroleum Engineering. His assistance and contributions, even though it was 12 hr difference in time zones, are highly appreciated. Also, I would like to thank KFUPM for allowing Dr. Patil to dedicate his time towards this effort while he is working there.

Also, I would like to express my gratitude to my parents for giving me continuous emotional and financial support during the past two and half years. I would like to thank James Choi for helping me with the experiments and Panav Hulsurkar and Neeraj Mahajan for the video recordings of the experiments. I would like to thank all my other friends for their words of wisdom and comfort during my hours of need.

Chapter 1 Introduction

1.1 Background

1.1.1 What is crude oil?

Crude oil is formed over millions of years by the decomposition of plants and animal material that have been subjected to burial due to overlaying of strata and sedimentation. Over the subsequent years, these deposits undergo transformation due to high temperature and pressures encountered in the earth's crust converting them into crude oil. This oil then migrates upwards from its initial position of formation towards the surface and becomes trapped in geological features where the deposit is capped by a non-porous, impermeable rock layer; this later becomes the oil reservoirs. The crude oil is then produced up to the surface by drilling wells that range from hundreds to thousands of feet deep. Once the oil is produced, it is then transported from the production sites to the storage facilities via pipelines (see Figure 1.1) or tankers.

Figure 1.1 Trans-Alaska Pipeline System

(Source: Alyeska Pipeline Service Company)

1.1.2 Major oil spills and their effects

Oil spills can occur during the production, transportation or storage of crude oil. Oil spills are a major environmental concern as is the disposal of water produced from oil wells. It is important to separate out the oil from the water as quickly as possible since oil spreads quickly on the water's surface. One ton of oil can quickly spread over a distance of 12 km. During the oil spill in the Gulf of Mexico, five million barrels of oil spread over an area of 75000 km^2. The current technologies fall short in acting at a rate required to prevent the oil spill from spreading (Pilipenko, Lerondeau, & Vial, 2013). Offshore oil spills affect the marine life on a large scale. While, if an oil spill were to occur on land, the oil would seep into the ground and contaminate the ground water (Spies et al., 1996).

(Vanem & Endresen, 2008) state that land based activities are a major contributor to the injection of oil into the marine environment which can be seen from the figure 1.2 shown below.

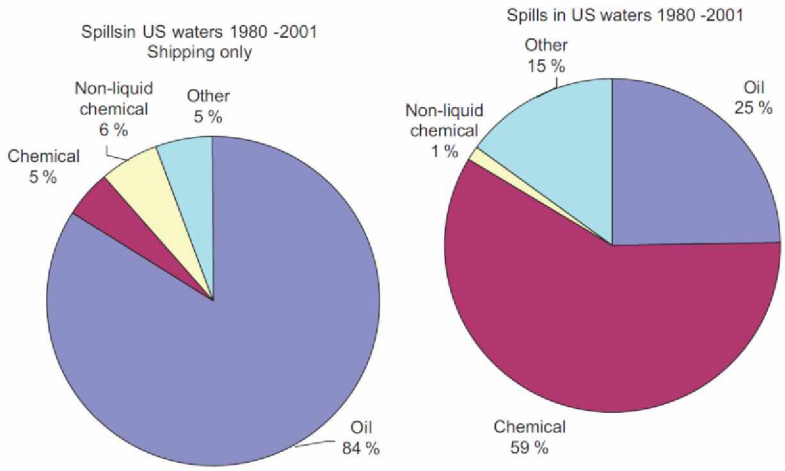

Figure 1.2 Spills in US waters between 1980 and 2001, shipping only (left) and including land-based activities (right) (Vanem, Endresen, & Skjong, 2008)

1.2 Objectives

This thesis focuses on evaluating the potential of iron oxide and graphene oxide nanoparticles as a medium of sorption for the uptake of crude oil from a marine environment. The objective of the study was to investigate the effect of encapsulation of nanoparticles in alginate gel, the concentration of nanoparticles and the contact time between the sorbent and the oil-water mixture on the efficiency of the nanoparticles to act as a successful sorbent for oil-water separation. Sorption was studied for iron oxide and graphene oxide nanoparticles at varying concentrations to determine optimum nanoparticle concentration. The nanoparticles were immersed in the oil-water mixture for a wide range of times to determine the optimal time when maximum uptake of oil could be achieved. The research is proposed to influence future oil spill response techniques that can reduce the response time required for spill clean-up along with an increase in the efficiency.

1.3 Hypotheses

1. The nanoparticles have a higher sorption capacity than orange peel particles and blank alginate capsules.
2. Increasing the contact time will increase the efficiency of nanoparticles to adsorb heating oil until a certain threshold or saturation is reached.
3. Graphene oxide nanoparticles will perform better in the sorption of oil than iron oxide nanoparticles.

Chapter 2 Literature Review

In this chapter, we will be looking at current techniques available for oil spill clean-up ranging from the use of sorbent materials, mechanical removal and modern techniques such as in-situ burning and bioremediation. We will also be looking in depth at the research that has been done on the use of nanoparticles as sorbents for heavy metals in treating water.

2.1 Alginate beads as an immobilization mechanism for sorbents

Alginate beads have been used as a method of immobilization for industrial microbiological purposes for some time now (Chen & Huang, 1988; De-Bashan, Moreno, Hernandez, & Bashan, 2002; Rocher, Bee, Siaugue, & Cabuil, 2010). The advantage alginate beads have is that they provide a porous medium for the encapsulated material to interact with the system as compared to the other techniques (Smidsrod & Skjakbrk, 1990). Alginate beads are considered an effective technique for the immobilization of living cells; the main reason for this being their inert nature and strong mechanical properties. The beads can be engineered to inherit various properties depending upon the molecular weight. Because of the high porosity of the alginate material, it is possible for the encapsulated material to interact with the environment without leaving the matrix structure. Another advantage of alginate beads is that they are non-harmful, making them ideal for living cell immobilization. However, along with the advantages that alginate beads have, they also have some drawbacks. They are highly susceptible to substances which have two Ca^{2+} ions. These substances react with the alginate beads destroying the bonds between the matrices and thus eroding the beads. The beads can, however, be manufactured in a one-step process by adding a Na-Alginate solution to a solution containing Ca^{2+} ions. The alginate

solution hardens into beads the instant it comes in contact with the calcium solution. This process will be further described in the next chapter.

2.2 Current methods for selective oil removal

As mentioned in chapter 1, nanoparticles are an up and coming technology for oil spill clean-up and will be discussed in further sections. Up until now, various techniques have been deployed for rapid and efficient oil spill response. These techniques can be classified into the following types: mechanical collection, chemical dispersants, in-situ burning, bioremediation, and sorbent materials. Most common offshore cleanup techniques are shown in Figure 2.1.

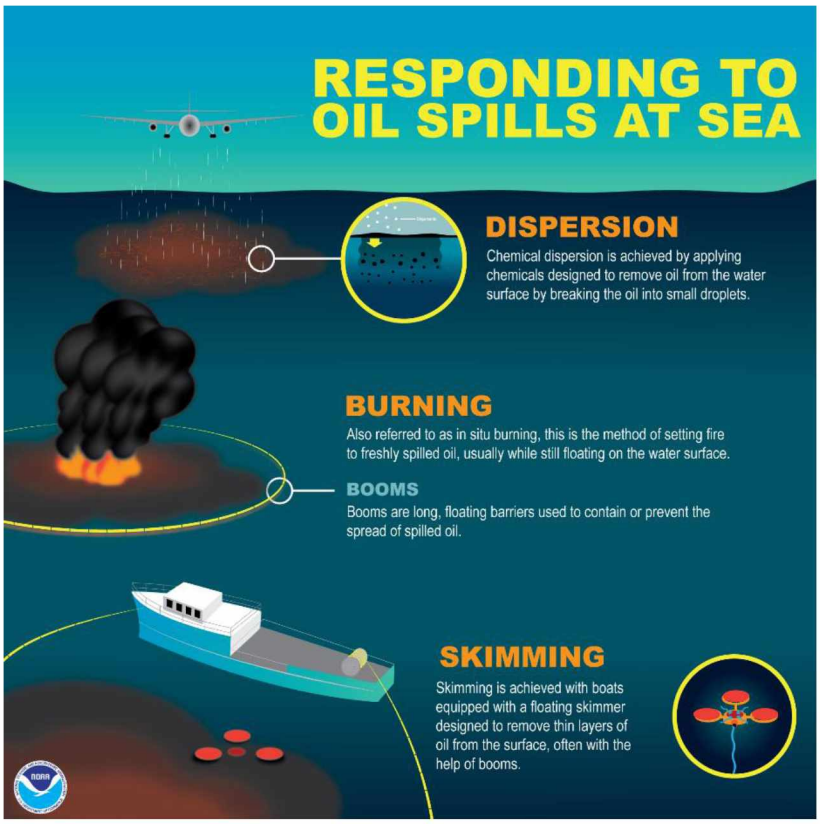

Figure 2.1 Responding to oil spills at sea

(Source: National Oceanic and Atmospheric Administration;

http://oceanservice.noaa.gov/facts/spills-cleanup.html)

2.2.1 Mechanical collection

Traditionally, mechanical collection has been the most used type of oil spill response (Broje & Keller, 2006). Skimmers and booms fall under mechanical collection. Of these, skimmers have been the most used oil recovery technique. The main principle behind the working of a skimmer is the tendency of oil to adhere to a rotating surface. When the oil comes into contact with the rotating surface, it is raised from the water surface and transported to a scraping device which in turn transfers it to a collector. In order to increase the efficiency of skimmers, they are deployed in various forms such as brush, disc, and drum. However, there are some drawbacks associated with using these kinds of skimmers. The recovery rate for skimmers is very low because of the small surface area that comes in actual contact with the oil. As only a low quantity of oil is recovered in each run, multiple runs need to be carried out; this results in an increase of time spent and therefore a higher cost. When the surface of the skimmer is changed to brushes or mops the recovery efficiency goes up for oil uptake; however, it becomes harder to recover the oil from these surfaces. All these drawbacks result in the need to develop a more efficient and more economical method of oil recovery.

Figure 2.2 A boom being deployed to contain oil

(Source: U.S. Coast Guard; http://response.restoration.noaa.gov/about/media/how-do-oil-spills-out-sea-typically-get-cleaned.html)

2.2.2 Bioremediation

Bioremediation as an oil spill clean-up technique received attention after the *Exxon Valdez* oil spill in March, 1989. Bioremediation makes use of microorganisms for oil spill clean-up. The microorganisms can be either naturally present or they can be cultured in labs and brought on site. These microorganisms use the oil as a carbon food source. Bioremediation requires certain conditions for an optimum function, such as: food source, oxygen, and nutrients in a proper environment (Hamza, Adly, & Afifi, 2008). The naturally occurring bacteria need to be stimulated in order for them to degrade the organics. The bacteria cause an oxidation reaction to degrade the hydrocarbons into carbon dioxide and water in the presence of oxygen, and the energy generated during this reaction propagates the growth of new bacteria. However, for bioremediation to give optimum results, the temperature of the environment needs to be in the range of 10 to 45 °C. The pH of the environment should be in the range of 6-8, which needs to be maintained as biodegradation results in the release of acid.

Liddell and Ramert (1994) performed experiments to determine the feasibility of bioremediation for clean-up of diesel range hydrocarbon spills in the Arctic regions.

2.2.3 Aerogels

Aerogels are synthetic, lightweight and porous materials derived from gels which have very high surface area per unit mass ratios (Kistler, 1932). By modifying the manufacturing processes, it was possible to develop aerogels with properties such as mechanical strength, flexibility, hydrophobicity and water stability. The aerogels were used for removing organic and inorganic solvents, oil and heavy metals from water (Reynolds, Coronado, & Hrubesh, 2001), (Standeker, Novak, & Knez, 2007), (Quevedo, Patel, & Pfeffer, 2009). Research was carried out on the use of aerogels as oil spill clean-up materials with results showing aerogels being able to adsorb up to 14 times their dry weight (Reynolds et al., 2001). By changing the material of manufacture, it was possible to achieve different properties in the aerogel matrix ranging from increased physical strength, fibrous texture and recyclability.

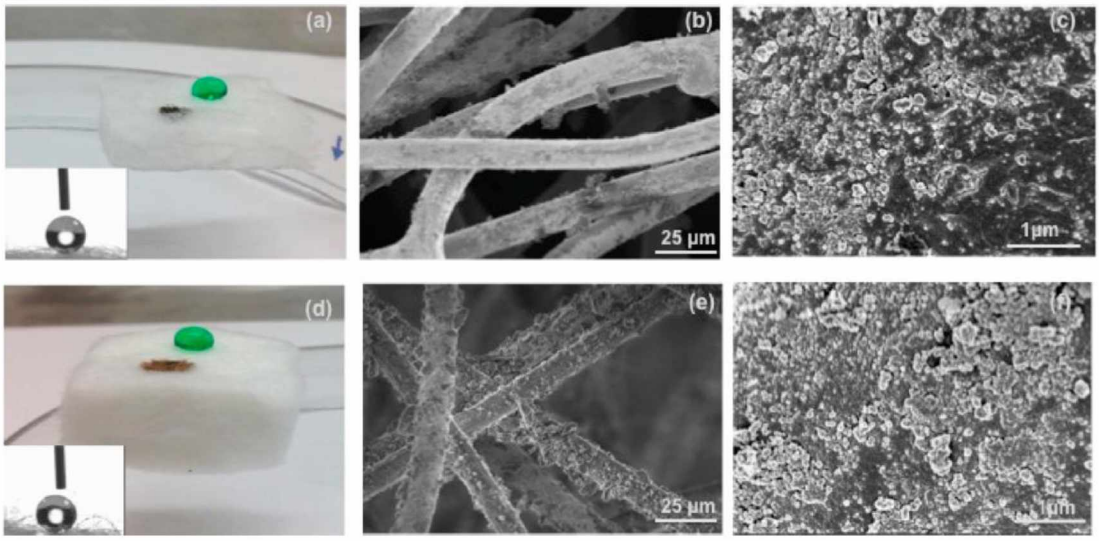

Figure 2.3 Optical interrogation of aerogel fabrics' gross and fine structure

Image of a dyed-green water droplet and Iraq oil on the surface of (a) TW (6 mm thick) and (d) SL (10 mm thick). Insets are images from the WCA measurements. Note that the TW used is thinner than SL. SEM images of the surfaces of (b and c) TW and (e and f) SL, where aerogel particles are visible on the fibers in the high-resolution images (c and f) (Karatum, Steiner, Griffin, Shi, & Plata, 2016)

2.2.4 In-situ burning

The research on in-situ burning began in the 1970s as an oil spill clean-up technique (Mullin & Champ, 2003). In-situ burning requires the use of special equipment such as fire booms, herders, and igniters in order to be carried out. However, it is possible to remove oil from a surface at very high rates. It has been used for oil spill clean-up for small water bodies and land spills. The use of this technique for marine clean-up is an issue of further research. The advantages associated with the use of in-situ burning includes the simplicity of the technique since it is easy on the logistical requirements, has high efficiency for oil removal at fast rates, and low costs. Research has proven that in-situ burning is successful in fresh, as well as salt water, bodies and can be used

in tropical and arctic conditions with similar results. There are, however, certain drawbacks associated with the use of burning as an oil spill clean-up technique. There is a chance of flashback occurring that could lead to a secondary fire causing extensive damage. Another drawback to burning oil is that the process may cause the initial product to undergo a change since the majority of the product is converted into gaseous constituents and the residue remaining can require specialized removal techniques (Fingas, 2011).

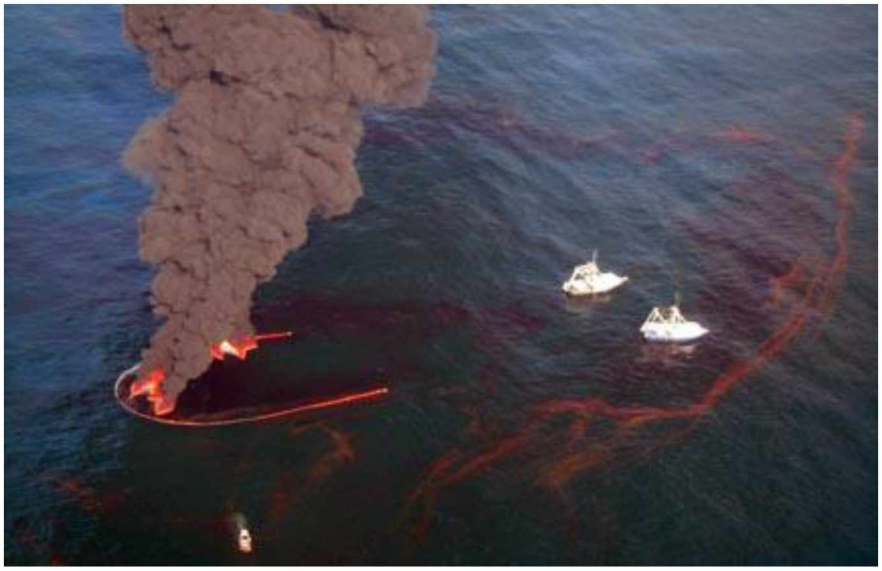

Figure 2.4 In-situ burning

(Source: U.S. Department of wildlife and fisheries

https://www.fws.gov/fire/news/national/oilBurns.shtml)

2.2.5 Dispersants

The principle on which dispersants work is that they chemically react with the oil, diluting it and dispersing it throughout the water column. It has the advantage of high rates of removal in comparison to a skimming operation since they can disperse a large amount of oil. However, they do have a massive drawback since they do not actually remove oil from the marine source. Dispersants disperse the oil from the water into the water column. The advantage of this is that it

prevents oil from reaching the shoreline and damaging coastal life, as well as preventing the spread of the oil over large marine areas. The drawback is that they do not remove the oil from the water; they just disperse it into the column, consequently posing a threat to the marine life and ecosystem within the water body. Hence, dispersants are deployed only when large oil spills are considered (Mullin & Champ, 2003).

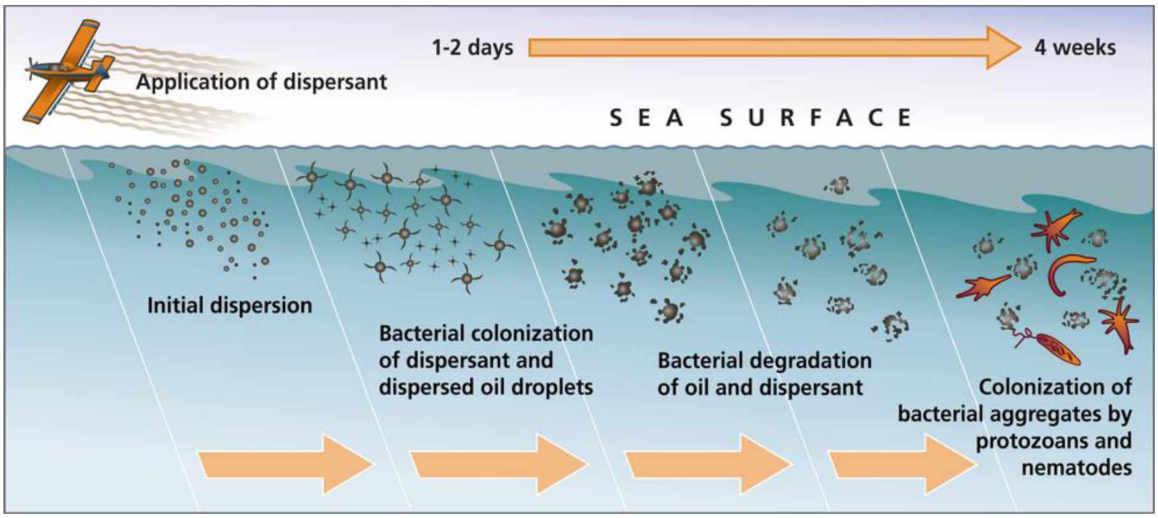

Figure 2.5 Dispersants work by dispersing oil into smaller droplets that can be consumed and degraded by bacteria (Prince, Lessard, & Clark, 2003)

Table 2.1 Summary of different methods of oil spill treatment

Technique	Application	Source
Booms and Skimmers	Low tides and calm water	(Broje & Keller, 2006)
Bioremediation	Temperature range of 10 – 45 C	(Hamza et al., 2008)
Aerogels	Low current and contained oil	(Reynolds et al., 2001)
In-situ burning	Low wind conditions	(Mullin & Champ, 2003)
Dispersants	Almost all kinds of open sea spills	(Mullin & Champ, 2003)

2.2.6 Sorbents

Sorbents are a new technology being deployed as an oil spill clean-up response. Graphene dioxide foams, nanocomposites, hydrogels, and carbon nanotubes all fall under this category. Sorbents perform on the principle of adsorbing the oil onto their surface. Some sorbents have been developed that can be reused, making them efficient and cost effective. The main disadvantage of using sorbents is the lack of actual field application that these three sorbents have during oil spills. Though they have a high rate of oil removal in experimental conditions, they seem to fall short when actual field conditions come into play. Also, manufacturing some of these adsorbents is a complex and sophisticated process that increases their overall cost of application.

Nanoparticles as an adsorbent material have gained popularity in recent years. Different kinds of nanoparticles perform different and specific kinds of functions. A few nanoparticles are discussed in the following section.

2.3 Nanoparticles as sorption agents

Nanoparticles have seen applications in the medical, chemical, and mechanical industries in recent years. Much research has been done in the field of water treatment where nanoparticles have been used as an adsorbent material for heavy metals such as Cadmium (Y. Feng et al., 2010), Zinc (Y. Feng et al., 2010) and Arsenic (L. Feng, Cao, Ma, Zhu, & Hu, 2012). They have also found use in the medical industry(Copland et al., 2004; Prabhu & Poulose, 2012; Xiao et al., 2012). Nanoparticles have a large surface area to volume ratio; this property enables them to adsorb a contaminant at multiple times the volume of the nanoparticles. This property of nanoparticles makes them an excellent choice for use as adsorbents in a wide variety of fields. Extensive research has been carried out on the use of iron oxide, graphene oxide, silver, titanium dioxide, and zero valent iron nanoparticles as adsorption agents.

2.3.1 Graphene oxide nanoparticles

Graphene has gained popularity recently as an excellent adsorption material for oil due to its hydrophobic nature. Hydrophobicity ensures that the graphene molecules do not adsorb water and have a higher affinity towards the contaminant material. It also possesses some other unique properties such as being the thinnest and the strongest material available currently (Castro Neto, Guinea, Peres, Novoselov, & Geim, 2009), (Rao, Sood, Subrahmanyam, & Govindaraj, 2009), (Y. Xu, Sheng, Li, & Shi, 2010). Graphene tends to have a high surface to volume ratio. The work done by D. Li, Müller, Gilje, Kaner, and Wallace(2008) shows that the use of graphene sheets as membrane filters have been highly effective in the removal of particles and in general water treatment.

Graphene oxide is a highly oxidized form of graphite (Carbon) and is produced by a process involving the exfoliation of graphite. Y. Zhu et al. (2010) have shown in their work that graphene

oxide, as compared to graphite, is a soft material and the oxygen group makes it an optimal solution for water treatment. An extensive study on graphene oxide has shown that it has better performance in cases of contaminant adsorption as compared to carbon nanotubes or activated carbon membranes (Kyzas, Deliyanni, & Matis, 2014). This was possible due to the comparatively less compact construction of the particles providing more contact area for the contaminant. However, the problems associated with the thin graphene films include their tendency to have low porosity and that they usually form aggregates when injected in water. By encapsulating the graphene particles in alginate beads, we hope to resolve these issues.

2.3.2 Silver nanoparticles

Silver has been studied extensively through the years for its application towards the medical industry. It has also been an important material for water treatment (D. Li et al., 2008). The work of Mthombeni, Mpenyana-Monyatsi, Onyango, and Momba (2012) has shown that due to the increased surface area of the silver nanoparticles, they have more reactive power along with improved catalytic properties and increased adsorption capacities. Silver nanoparticles are amongst the most widely used nanoparticles, finding applications as an antimicrobial agent with over a hundred consumer products. In recent studies, the adsorbent qualities of silver nanoparticles have been tested on numerous contaminants, but the experiments have mainly focused on column experiments to remove *Escherichia coli* (Mthombeni et al., 2012; Quang et al., 2013). However, the toxicity of the silver nanoparticles is not fully understood with further studies required in order for wide scale application of the silver nanoparticles in water treatment..

2.3.3 Titanium dioxide nanoparticles

Titanium dioxide is the most studied of the nanoparticles due to its photocatalytic properties, making it excellent for contaminant removal from both water and air (Q. Li et al., 2008). This nanoparticle is capable of killing gram-negative, as well as gram-positive, bacteria (Li et al., 2008). More recently, these nanoparticles were reported to kill viruses such as *poliovirus* 1, hepatitis B, Herpes simplex, and MS2 bacteriophage (Q. Li et al., 2008). Silver or gold doped titanium dioxide has also shown a great deal of promise by greatly improving the ability of these nanoparticles to inactivate bacteria and viruses (Q. Li et al., 2008). Silver is believed to enhance photoactivity, and gold is effective at degrading and mineralizing organic compounds (Ayati et al., 2014). Currently, TiO_2 is used in products such as sunscreen, toothpaste, paints, and air purifiers. There are even industrial scale water purification systems that utilize this nanoparticle as a photocatalyst (Q. Li et al., 2008). Similarly, TiO_2 holds a great deal of promise in water treatment since it is stable in water, non-toxic by ingestion, and relatively inexpensive (Q. Li et al., 2008). With further study of these particles, titanium dioxide may prove to be extremely useful for small scale water treatment.

2.3.4 Zero-valent iron nanoparticles

nZVI (nano zero valent iron) nanoparticles have already proven to be useful in the removal of various groundwater contaminants. nZVI were injected into aquifers in order to remove chlorinated compounds, pesticides, and heavy metals, as well as explosives that may be present in the groundwater source (Krajangpan, Jarabek, Jepperson, Chisholm, & Bezbaruah, 2008). These applications have been used since the 1990s, and recently there has been more interest in the zero-valent iron nanoparticles (Kim, Hong, Jung, Kim, & Yang, 2010). There are concerns as to the fate

and transport risks that are involved when nZVI are injected into water sources, requiring immobilization techniques in order to eliminate this risk (Kim et al., 2010).

nZVI have been studied in multiple batch experiments in order to test their removal of trichloroethylene (TCE) (Kim et al., 2010; Krajangpan et al., 2008), as well as nitrate (Krajangpan et al., 2008). Removal of TCE was found to be around 90% in two hours, following pseudo first order kinetics (Bezbaruah, Shanbhogue, Simsek, & Khan, 2011) or 99.8% following the same kinetics (Kim et al., 2010). In general, nZVI were found to be extremely efficient at the removal of the chlorinated solvent. Experiments involving nitrate demonstrated a 55-73% removal of bare nZVI and 50-73% removal with entrapped nZVI over a two-hour period. This experiment proved that entrapped nZVI are just as reactive as those not enclosed in alginate, and efficiency may, in fact, be increased with particle entrapment (Krajangpan et al., 2008). Each of these experiments gave a significant case for the use of entrapped nZVI for use in groundwater remediation (Bezbaruah et al., 2011; Krajangpan et al., 2008) or in dehalogenation of chlorinated solvent (Kim et al., 2010).

2.3.5 Iron Oxide nanoparticles

Iron oxide nanoparticles have gained popularity with a wide range of research being conducted on their synthesis and use. They exhibit a unique range of properties, such as high surface area to volume ratios and superparamagnetism (Afkhami & Moosavi, 2010; McHenry & Laughlin, 2000; Pan, Chiou, & Lin, 2010). The iron oxide nanoparticles have a very simple synthesis process (Palchoudhury & Lead, 2014) and the ability to be coated with different materials to impart a multitude of specific properties (Boyer, Whittaker, Bulmus, Liu, & Davis, 2010; Dias, Hussain, Marcos, & Roque, 2011). It was possible for Palchoudhury and Lead (2014), to develop a simple yet effective method of manufacturing magnetized iron oxide nanoparticles that could be

used in the separation of oil from an oil-water mixture. The authors were able to synthesize polyvinylpyrrolidone coated iron oxide nanoparticles which were then capable of selectively adsorbing oil. This research not only proved the capability of iron oxide nanoparticles as sorbents, but it also established them as a potential medium for selective oil removal from an oil-water mixture. Considerable research on the use of iron oxide nanoparticles as heavy metal sorbents for wastewater treatment has already been carried out (P. Xu, Zeng, Huang, Feng, et al., 2012). These studies have established iron oxide nanoparticles as a cost effective and efficient adsorbent for heavy metal and oil removal.

Table 2.2 Research conducted on different nanoparticles as sorbents for water contaminants

Batch/Col	Nanoparticle	Contaminant	Source
Packed bed column	Silver	*Escherichia coli*	(Cai et al., 2012)
Fixed bed column	Silver	*Escherichia coli*	(Mthombeni et al., 2012)
Filter column	Silver NP silica	*Escherichia coli*	(Quang et al., 2013)
Column	Surface modified iron	Arsenite	(Giasuddin, Kanel, & Choi, 2007)
Batch	Zero-valent iron	Trichloroethylene	(Lee, Kim, Lee, Shin, & Yang, 2009)
Batch	Graphene oxide	Copper	(Algothmi, Bandaru, Yu, Shapter, & Ellis, 2013)
Batch	Zero-valent iron	Nitrate	(Krajangpan et al., 2008)
Batch	Zero-valent iron	Trichloroethylene	(Bezbaruah et al., 2011)
Batch	None/ alginate beads	Silver and Gold	(Torres et al., 2005)
Batch	Graphene oxide	Acridine orange	(L. Sun & Fugetsu, 2014)
Batch	Iron Oxide	Crude Oil	(Palchoudhury & Lead, 2014)

2.4 Effect of temperature on adsorption by nanoparticles

Temperature plays an important role in the adsorption process. According to Ten Hulscher and Cornelissen (1996), current literature available on the influence of temperature on sorption describes its effect on sorption equilibrium. The author studied a wide variety of solutes and sorbing materials, and found that slow as well as fast sorption reaction depended on the temperature of the experimental environment. Ten Hulscher and Cornelissen (1996), discovered that the sorption equilibrium depended on the enthalpy of the overall reaction, with sorption at equilibrium decreasing with increasing temperature. Shipley, Yean, Kan, and Tomson (2009), conducted experiments for the adsorption of arsenic onto magnetite nanoparticles. Here they studied the effect of temperature on the overall sorption of arsenic over a temperature range of 20 to 30 °C. The experimental results showed that the adsorption was higher at 25 and 30 °C than at 20 °C indicating a higher adsorption at higher temperatures. Mak and Chen (2004), carried out experiments on the adsorption of methylene blue on modified iron oxide nanoparticles. According to the authors, the results obtained indicated that an increase in temperature resulted in an increase in the adsorption of methylene blue, Thus, the literature indicated that, in the case of nanoparticles, an increase in temperature resulted in an increase in the adsorption capacity. In this research study, the temperature was maintained at 25 °C and no comparison studies at different temperatures were carried out.

2.5 Effect of salinity on adsorption by nanoparticles

Salehi, Arami, Mahmoodi, Bahrami, and Khorramfar (2010), carried out research on the effect of the presence of inorganic salts on the dye adsorption characteristics of modified zinc oxide nanoparticles. Based on their results, the authors were able to conclude that the presence of salts decreased the sorption capacity of the nanoparticles with a decrease of almost 20%.

Mirshahghassemi and Lead (2015) carried out research involving the recovery of oil from water under environmentally relevant conditions. In their research, the authors used seawater to measure the effect of salinity on the adsorption characteristics. The authors do not mention the exact comparison in the removal percentages; however, Mirshahghassemi and Lead do mention that a higher quantity of nanoparticles was required to remove a similar quantity of oil when SRFA (Suwannee River Fulvic Acid) was added to the oil – water mixture. Thus, the available literature indicates that an increase in the salinity of the experimental environment decreases the adsorption capacity of nanoparticles. Salinity comparison studies were not carried out in this research. All experiments were carried out using deionized water.

Chapter 3 Methods and Materials

In this research, three sorbents materials (orange peels, iron oxide nanoparticles, graphene oxide nanoparticles) were tested for adsorption efficiency for two adsorbates (methylene blue and heating oil no. 2) by conducting the following bench-scale tests.

Table 3.1 List of experimental runs carried out as a part of this research

Adsorbate	Adsorbate Quantity	Sorbent	Sorbent Quantity	Analytical Instrument
Methylene Blue	50, 100, 200, 300, 400, 500 mg/L	Orange Peels	1, 2, 3, 4, 5 g/L	UV-vis
		Iron Oxide Nanoparticles	1, 2, 3, 4, 5 g/L	
Heating Oil #2	200 mg/L	Orange Peels	4, 5 g/L	UV-vis, GC/MS
		Iron Oxide Nanoparticles	1, 2, 3, 4, 5 g/L	UV-vis, GC/MS, Fluorescence Spectroscopy
		Graphene Oxide Nanoparticles	1, 2, 3 g/L	

In order to prevent the sorbents from dispersing into the solution, it was decided to encapsulate them into alginate beads. The process for encapsulating the sorbents is explained in the following section.

3.1 Formation of alginate beads

A similar process as described by De-Bashan et al. (2002) has been used in forming the alginate beads. Sodium alginate was added to ultrapure water at a concentration of 10g/L. Care was taken while mixing the sodium alginate as sodium alginate congeals into clumps when it is added to water. The mixture was continuously kept agitated to achieve a uniform solution. A calcium chloride solution was prepared by adding $CaCl_2$ to ultrapure water at a concentration of 3.75g/L. The beads were obtained by adding sodium alginate solution to the calcium chloride solution dropwise. As soon as the alginate entered the calcium chloride solution, it solidified into a hard bead form. The beads were left in the solution overnight for reverse osmosis to remove excess water and for the beads to achieve a stable form. The beads obtained by using this process are quite durable and can be used to carry the intended adsorbent to the target location. However, the drawback of using sodium alginate to create the beads is that they will easily disintegrate if the target environment is Ca^{2+} rich.

The adsorbent is embedded into the beads by adding it to the alginate solution and then proceeding to manufacture the beads using the above process. The advantage of using alginate beads as carriers is that the beads have a matrix-like structure. Since they are a porous media through which the adsorbent can interact with the contaminant, this makes them ideal for oil-water separation applications. Additionally, the pores were small enough to prevent the adsorbent from dispersing into the target water body. Once the adsorption process was complete, the beads were easily recovered by passing the water and oil solution through a filtration device aiding in the easy recovery of the nanoparticles. This prevented contamination of the target water body by nanoparticles and helped in their recovery for multiple uses.

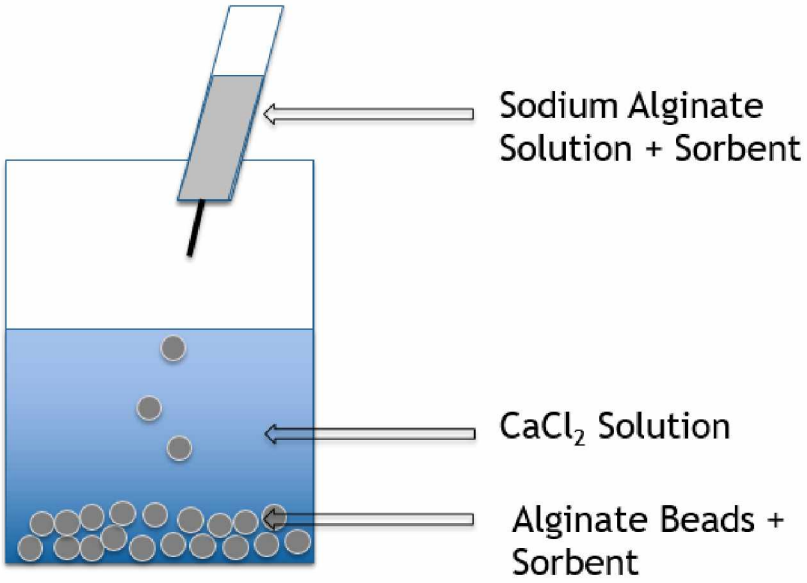

Figure 3.1 Formation of alginate beads

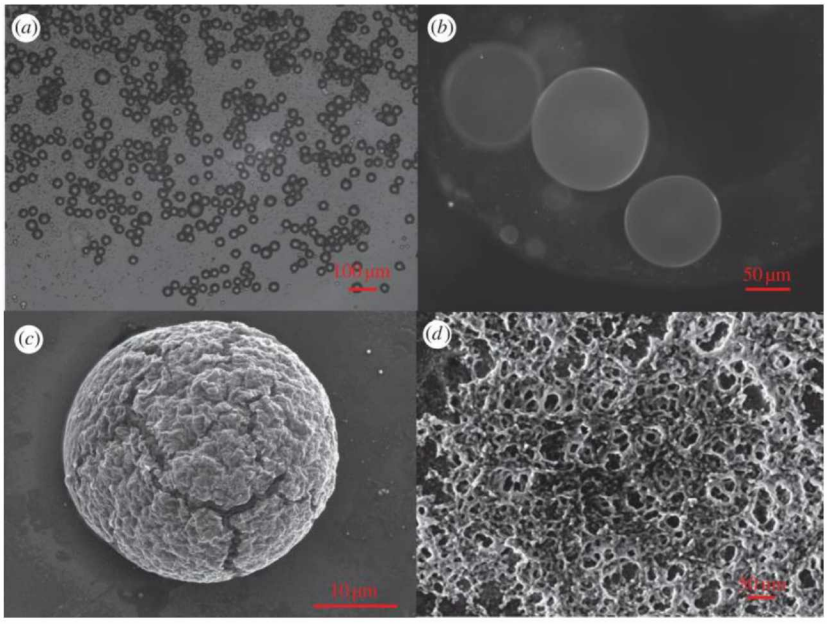

Figure 3.2 (a) Alginate gel microspheres (diameter: 30 µm) with immobilized antibodies (b)fluorescence image of alginate microspheres (diameter: 60 µm) (c,d) scanning electron microscopy (SEM, Sirion, FEI, 5kV) images of alginate microsphere

(Karatum et al., 2016)

3.2 Sorbents

The initial experiments were carried out using orange peels as the adsorbent. The powdered orange peels were custom made in house. Store bought oranges were used for the purpose. The orange peels were flash frozen to -81° C and vacuum dried for 24 hours. Then the vacuum dried peels were ground and sieved using Mesh no. 10 to obtain 2 mm orange peel particles. The iron oxide nanoparticles were bought from Sigma-Aldrich (Aldrich 544884) with a particle size of 50 nm. The graphene oxide nanoparticles were produced in-house as well (T. Chowdhury, L. Zhang; unpublished work).

3.3 Sample preparation and testing

In order to be able to observe the change in oil concentration, it was decided to use a heating oil concentration of 0.5 g/L (500 ppb). However, it was found that heating oil was not miscible with water. It is necessary to achieve a uniform distribution of the contaminant in water for the beads to be able to adsorb the oil. Methanol was then used as a buffer between heating oil and water. Methanol is able to dissolve a small amount of heating oil and is easily dispersed in water, making it easier for the heating oil to be easily distributed in water. A stock solution of oil and methanol was prepared by adding 250 µL of heating oil to 40 mL of methanol. 1 L samples were prepared by spiking 1 L of ultrapure water with 40 mL of the stock solution. Once the samples were prepared, the alginate beads (with set amount of adsorbent) were added to the sample. Beads were added to the sample, and the solutions were kept on a shaker table at a speed of 240 rpm and a temperature of 25 °C was maintained for the duration of the experiment. Adsorption was measured for the following time steps: 10 min, 20 min, 35 min, 50 min and 70 min.

3.4 Quality assurance and controls

At this point, a quality control needed to be established in order to ensure that the data that we would obtain from the experiments would be considered as valid. To meet this end, two primary controls were established. The first control was to measure the evaporative loss of heating oil that might take place during the course of the experiment. To study this parameter, blank samples were prepared that contained only oil and water emulsion. These solutions were put through the same process mentioned above with the exception of adding any nanoparticles or alginate beads to them. Analyzing these solutions would then provide us with the amount of evaporative loss that might take place during the experiment. The second control was to measure accurately the quantity of oil that was adsorbed by the alginate beads and not by the nanoparticles themselves. To establish this control, blank alginate beads with no adsorbents were prepared. These were then added to the oil-water solution and were processed as mentioned above. The analysis of the resulting solution provided us with the quantity of oil that was lost to adsorption by the alginate beads without actually reaching the nanoparticle.

3.5 Extraction of oil from water

A GC-MS (Gas Chromatography and Mass Spectroscopy) instrument was used to analyze the concentration of oil remaining in the water after the adsorption process was completed. Gas Chromatography instruments are highly sensitive to water and can be damaged by water vapors. Hence, it became necessary to extract the oil in the sample from the water. Dimethyl chloride (VWR) was used for this purpose. Dimethyl chloride was observed to be an excellent adsorbent for hydrocarbons since it was immiscible in water. 200ml of dimethyl chloride was added to the samples in a separatory funnel and processed for 10 min. The dimethyl chloride obtained this way was our final extract laced with the residual oil after the adsorption had been completed. This

process was repeated for each sample. Once the hydrocarbon infused dimethyl chloride was obtained, the extract was concentrated to a 1 ml concentrate by evaporating the dimethyl chloride in a rotary evaporator (Buchi RotoVaporator R-300). Once the final concentrate was obtained, it was analyzed in the GC-MS for hydrocarbon content.

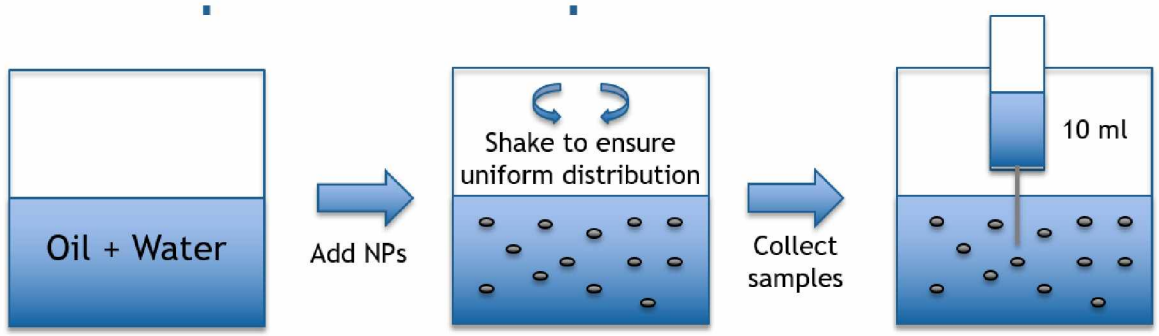

Figure 3.3 A schematic of the experimental process GC-MS method

The injection column (HP5MS 30 M x 0.32 mm 0.25-micron film thickness) pressure was set at 20 psi, and the temperature was set at 40 °C for two minutes. Once the preset temperature was reached, a temperature increase was set at a rate of 12 C/min until it reached 320 °C. The column was then maintained at this temperature for about 15 min for an expected run time of approximately 36 min. The FID (flame ionization detector) was set at a detector temperature of 320 °C and an injector temperature of 280 °C. The column was then able to separate diesel range organics from the internal standards and methylene chloride (surrogate). Therefore, the resolution for methylene chloride solvent was set from C_{10}. Since the concentration of DRO (diesel range organics) was low in the samples, a pulsed DRO method was proposed. The advantage of using a pulsed injection method was that it was able to push low concentration of solute at high pressure through the column, aiding in the proper detection of the hydrocarbon components.

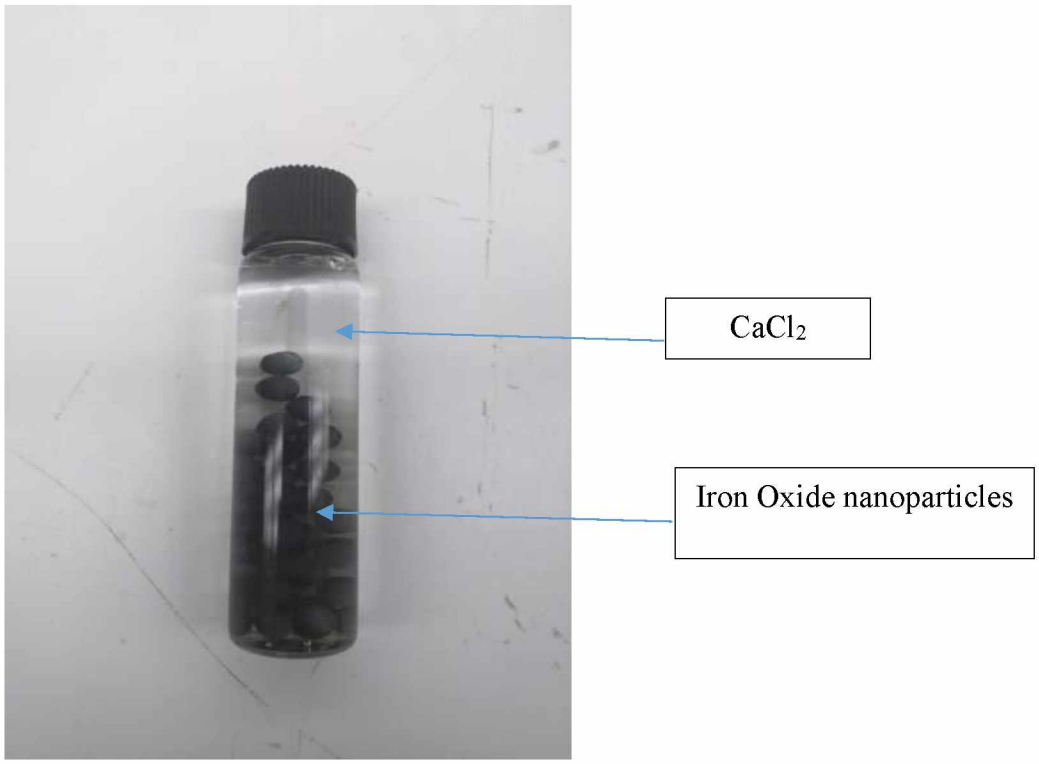

Figure 3.4 Iron Oxide nanoparticles encapsulated in sodium alginate beads

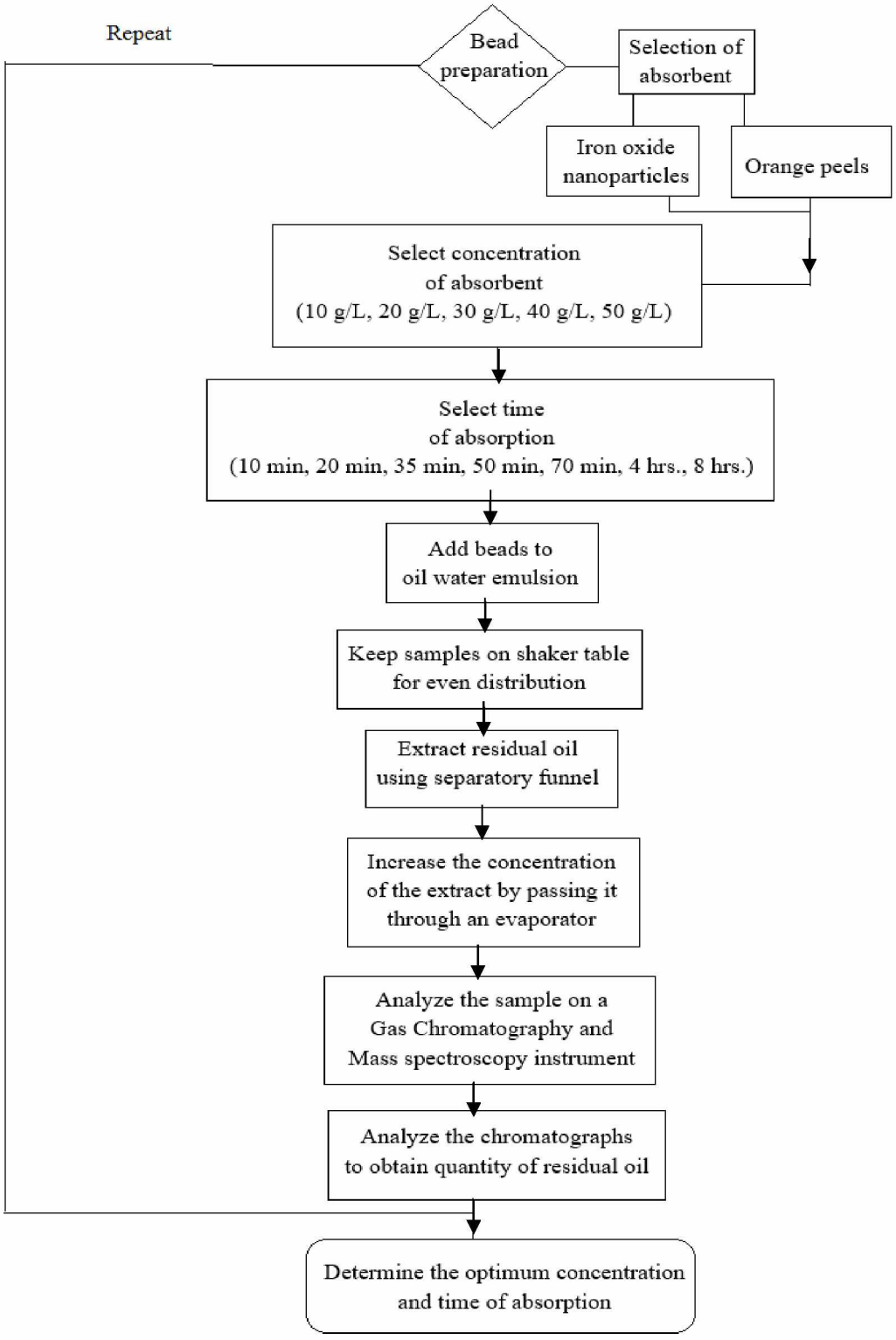

Figure 3.5 Flow process of the experiment

Chapter 4 Results and discussion

In this chapter, we will discuss the results obtained after performing the experiments mentioned in Table 3.1. After analysis of the data obtained from the GC/MS, it was found that orange peels were able to only remove 10% of the initial oil in the oil-water mixture, iron oxide nanoparticles were able to remove 77%, and graphene oxide nanoparticles were able to remove 81% of the oil. The results are explained in the next sections.

4.1 Sorption of methylene blue using orange peels

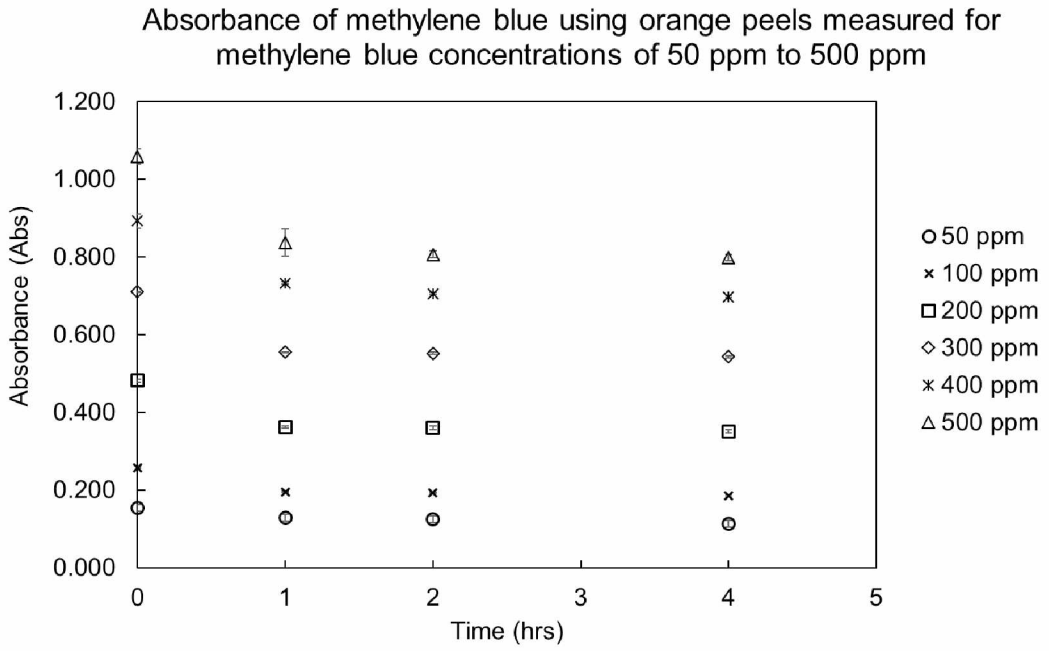

Figure 4.1 Adsorbance of methylene blue using orange peels measured for methylene blue concentrations of 50 ppm to 500 ppm

In order to determine the effectiveness of orange peels as a medium of sorption, it was decided to test them for the sorption of methylene blue. A set of 6 concentrations of methylene blue ranging from 50 ppm to 500 ppm were used for this analysis. The alginate encapsulated

orange peels were then kept in the solution for the duration of 1 hour, 2 hours, 3 hours and 4 hours respectively. Samples were collected from the solutions at the above-mentioned time intervals, and the adsorbance values were recorded using an UV-vis. It must be noted here that the adsorbance value of ultrapure water is 0 Abs (the unit of adsorption value), so any impedance in the path of the ultraviolet rays is recorded as an increase in adsorbance value. From Figure 4.1 it can be observed that the methylene blue concentration goes on decreasing as the time for which the gel encapsulated orange peels are kept in the solution is increased. The next observation that can be made based on the data is that, as we increase the concentration of methylene blue in the solution, it does not seem to affect the uptake at a significant value with a similar amount of methylene blue being sorbed at increasing concentrations. However, it is also observed that after the 4-hour mark the adsorbance value slightly increases as compared to the previous values. This can be attributed to the saturation of the alginate beads which causes them to release some of the sorbed methylene blue back into the solution resulting in an increased adsorbance value for the various methylene blue concentrations

4.2 Analysis of sorption of heating oil by iron oxide nanoparticles using UV-vis spectroscopy

Once the experiments involving powdered orange peels and methylene blue were conducted, we moved towards experiments involving heating oil. The first method of analysis we used for the residual heating oil in the solution was UV-vis spectroscopy. Figure 4.2 shows the performance of the five concentrations of iron oxide nanoparticles over a period of eight hours. After comparing the residual oil concentrations of heating oil in the five samples, it was observed that the 2 g of NPs per liter of heating oil and water mixture produced the most optimal results. The absorbance value of heating oil in the solution went from an initial 25 Absorbance to 4.8

Absorbance in the first 10 min reached a minimum value of 4.6 Abs in 20 min which remained constant throughout the duration of the experiment. Compared to the other iron oxide nanoparticle concentrations, the 2 g was able to achieve a steady and immediate removal of the heating oil while maintaining the concentration at the same level as opposed to other concentrations where the heating oil secreted back into the solution. Hence, it was decided that the 2 g/L concentration of Iron Oxide nanoparticles was the optimal concentration for the removal of heating oil from the oil and water mixture. These results will be established in later sections by analyzing the residual oil using Gas Chromatography.

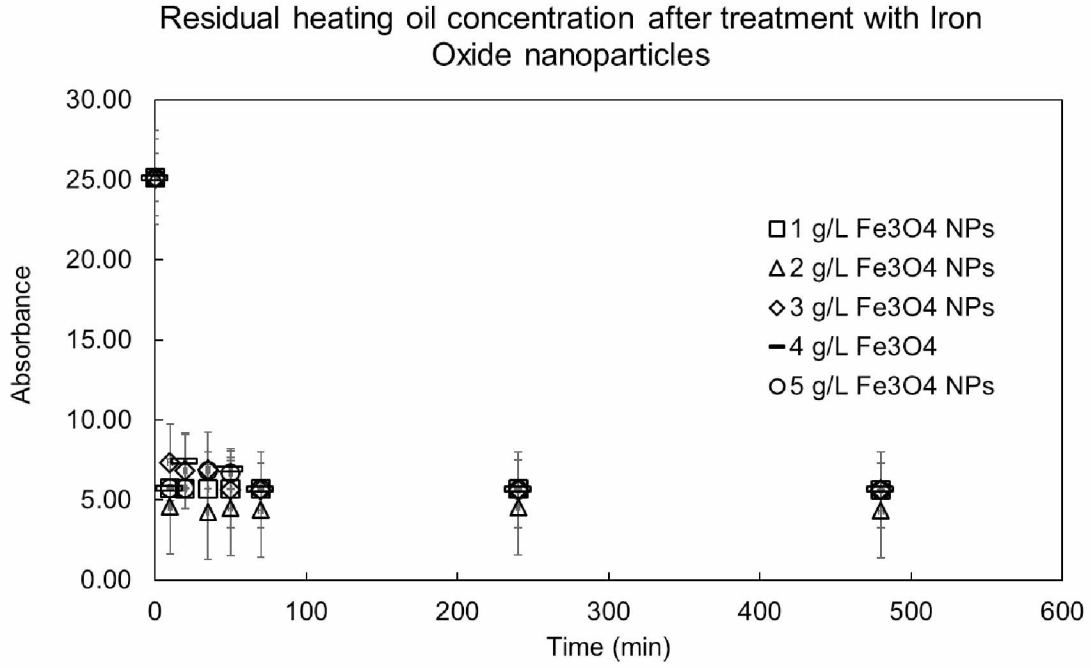

Figure 4.2 Concentration of residual heating oil after it was treated with 5 concentrations of iron oxide nanoparticles encapsulated in alginate beads over a period of 8 hours

4.3 Generation of calibration curve for heating oil experiments

A standard data curve was required in order to determine the concentrations of the residual oil remaining in the samples after they were treated with the gel encapsulated nanoparticles. The

standard curve data was used to develop the curves shown in Figure 4.5. In order to obtain the standard curve, the chromatographs showed in Figure 4.3 and Figure 4.4 were used. When a hydrocarbon or a mixture containing hydrocarbons is processed in a GS/MS it will produce chromatographs similar to those shown in the figures. In these particular experiments, d5-nitrobenzene and d8-napthalene were used as internal standards with 10 µl of each added to every sample before it was analyzed on the GC/MS. The internal standards appear on the chromatograph as high-intensity peaks whereas the grassy area represents the diesel range organics (DRO) or the hydrocarbons in the sample solution. The area under the total chromatograph corresponds to the quantity of heating oil added to the sample solution of heating oil and water, and it can be used to establish a standard curve. The method used in this research to develop the standard curve is explained in the next section.

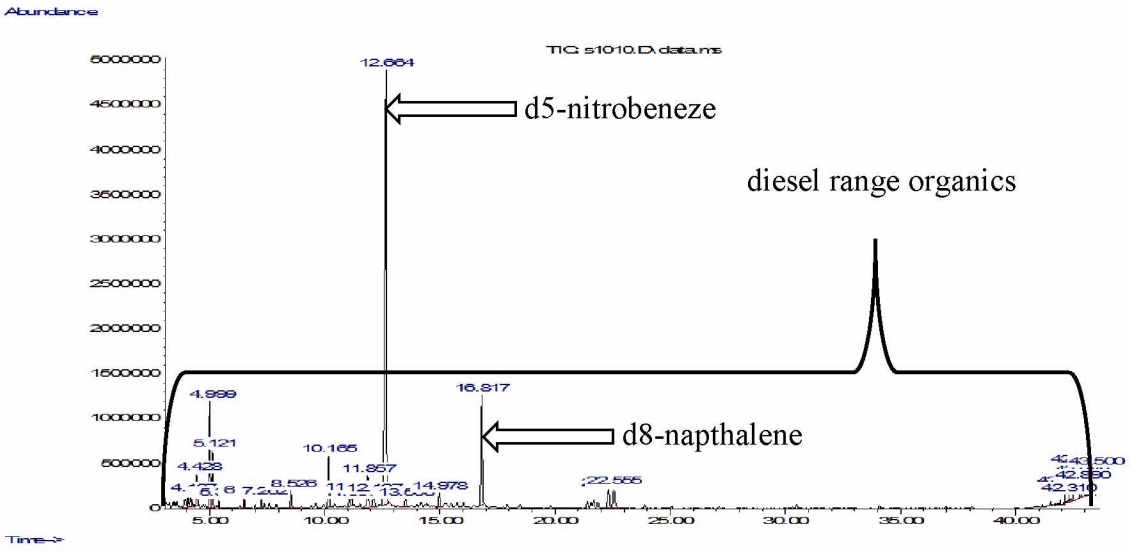

Figure 4.3 Gas Chromatograph for residual heating oil number 2 with a concentration of 40 mg/L

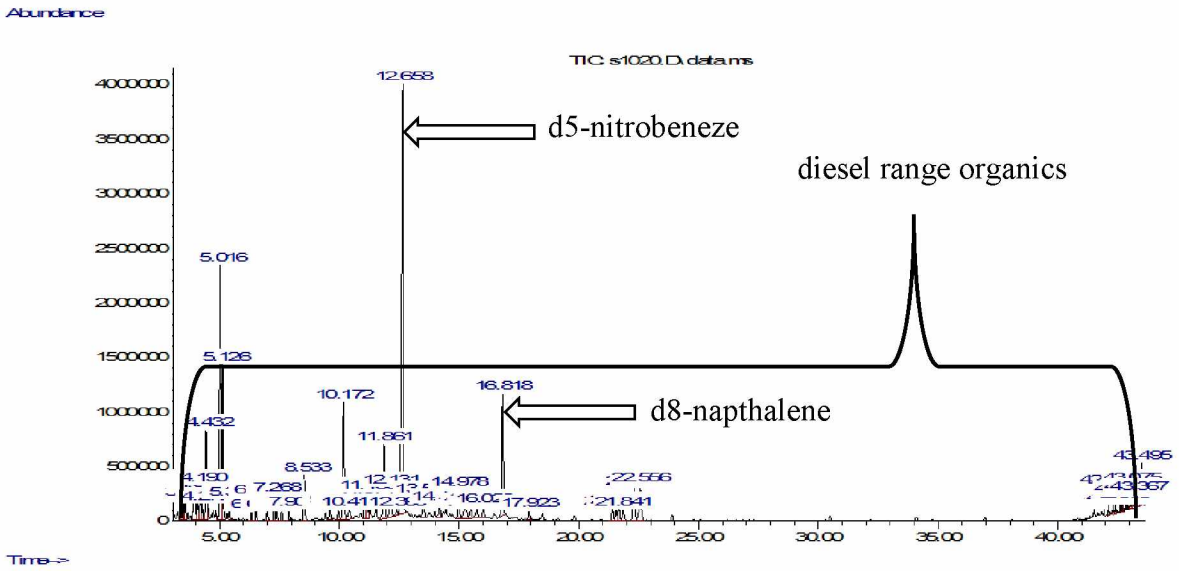

Figure 4.4 Gas Chromatograph for residual heating oil number 2 with a concentration of 60 mg/L

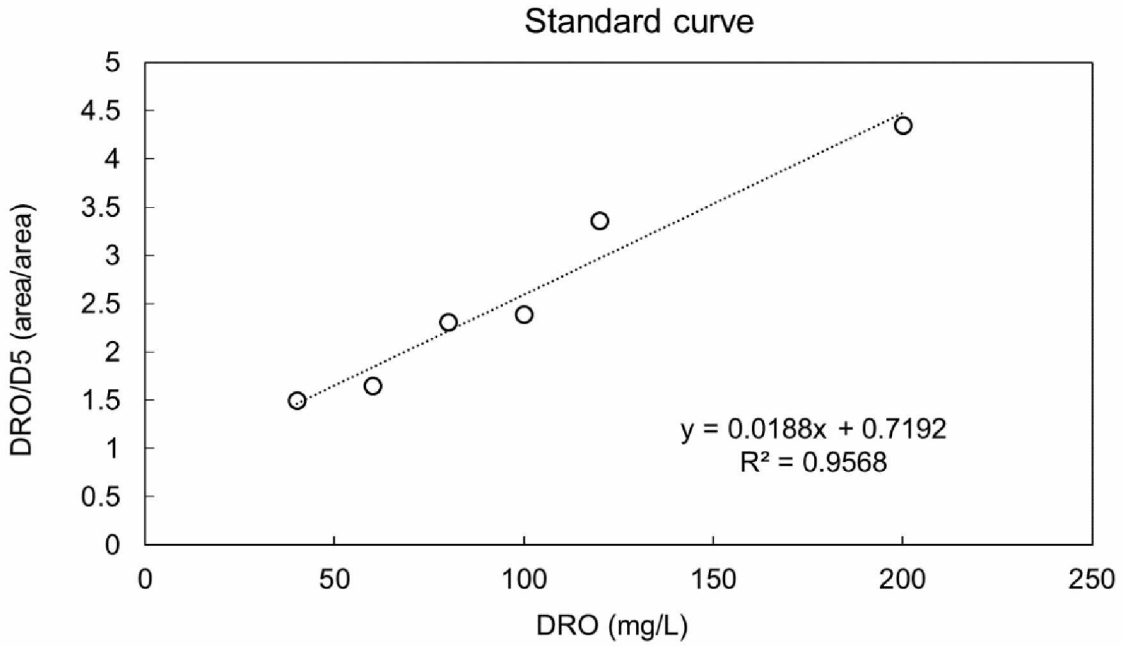

Figure 4.5 Standard curve developed by dividing the diesel range organics total area by the d5-nitrobenzene area

To develop the standard curves, standards with concentrations of 40, 60, 80, 100, 120 and 200 mg/L of concentration were prepared by adding the above concentration heating oil to 1 liter of deionized water, which were then analyzed using the Gas Chromatography & Mass

Spectroscopy instrument. This instrument develops a chromatograph where each hydrocarbon detected is translated into a peak, the height of which depends on the concentration of that particular hydrocarbon in the sample. The total area of each curve provides the concentration of each standard in terms of area. Dividing the total areas of the standards by the area of D5-nitobenzene, internal standard, yield the ratio value that can be used to generate a standard curve as shown in Figure 4.5

4.4 Using standard curve to calculate the residual oil concentration

A straight line can be fitted to the standard curve to obtain the slope and intercept. Once the samples are analyzed on the GC/MS, the ratio of the total area of the heating oil is divided by the area of the d5-nitrobenzene peak. Plotting a curve of the ratio vs. the area of heating oil will generate the standard curve, which can then be fitted to an equation to generate the standard curve equation. It was observed that the standard curve is a straight line which can then be used to calculate the residual oil or diesel range organics concentration. These concentrations can then be plotted accordingly against time to develop a sorption curve.

4.5 Evaluation of loss of sorbate (heating oil) due to evaporation

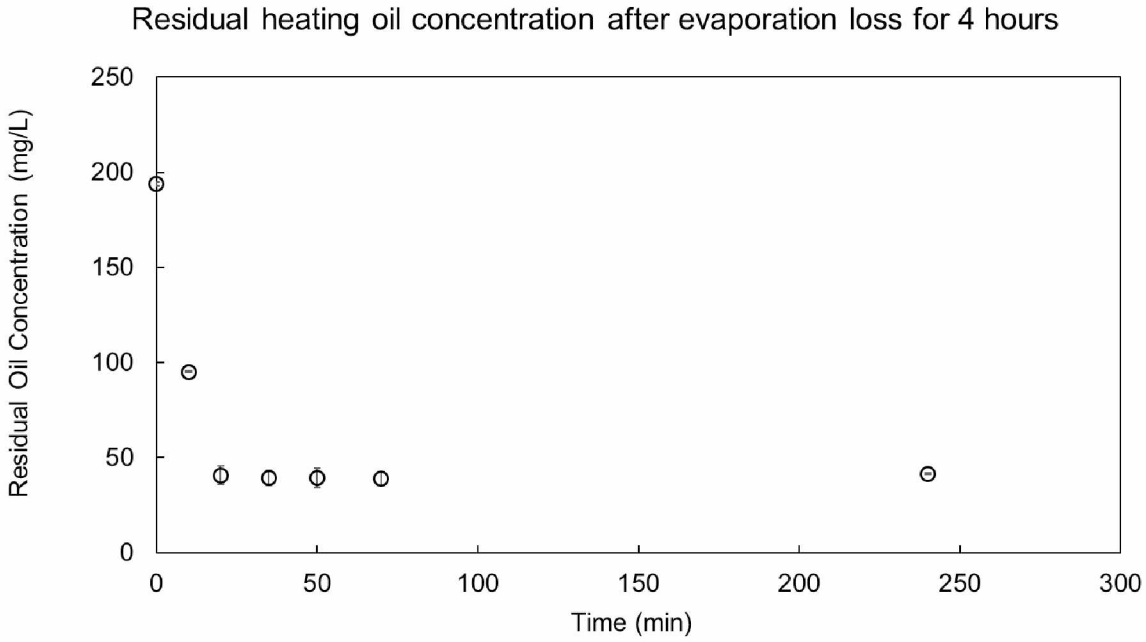

Figure 4.6 Concentration of heating oil remaining in the sample with respect to due to evaporation loss

Heating oil is a volatile substance and quite different from an actual crude oil which has a range of components varying from volatile to non-volatile that cannot be removed by evaporation alone. Heating oil consists of only lighter components and can easily evaporate when exposed to the atmosphere. Hence, during the entire process of the sorption experiments, it was necessary to prevent the heating oil in the sample solution from being lost due to evaporation. Precautions were taken during each experiment to enclose the sample in sealed containers to prevent evaporative loss. However, it became necessary to establish a control on the entire experiment to determine the exact evaporative loss taking place during the entire process. To obtain these parameters, an experiment was designed in such a way that evaporation loss was allowed within the duration of the process. Figure 4.6 depicts the loss of heating oil taking place over the time steps of 10 min,

20 min, 35 min, 50min, 70min, and 4 hours respectively. It was observed that the concentration of heating oil went from 200 mg/L present initially in the solution, to 98 mg/L inside 10 min. In 20 minutes the concentration reduced to 46 mg/L after which the concentration remained almost constant. This suggested that even with volatile components, it was not possible for the heating oil to be completely removed from the water system due to evaporation alone, thereby requiring additional treatments in order to remove the heating oil from the system under consideration.

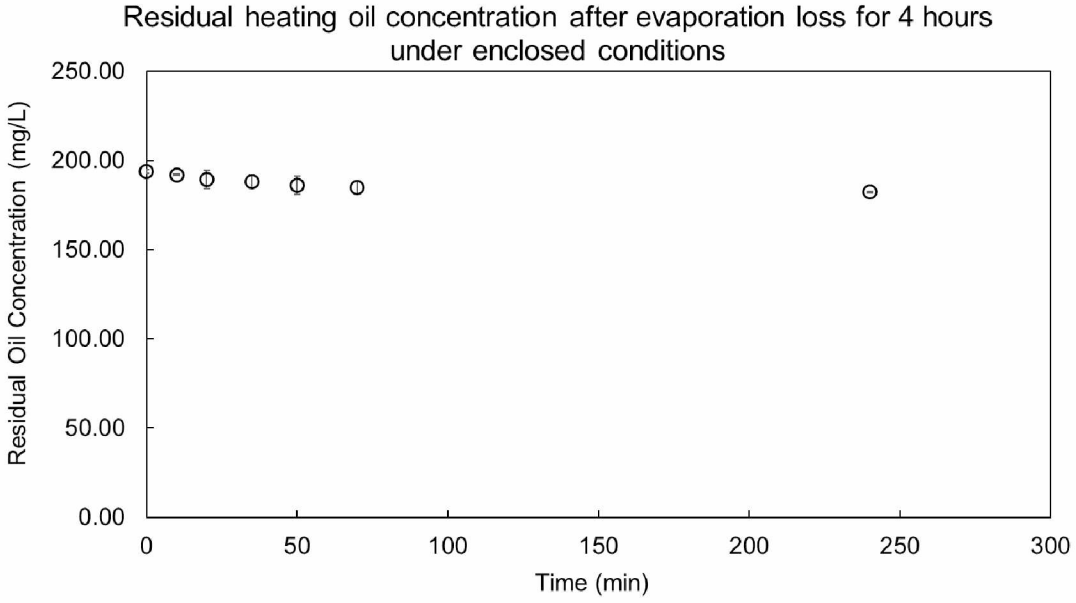

Figure 4.7 Concentration of heating oil remaining in the sample with respect to due to evaporation loss under enclosed conditions

Along with the experiments to determine the amount of heating oil lost due to evaporation, it was imperative for us to establish that under enclosed conditions the amount of heating oil lost was less than 10 % in order for the experimental conditions to be considered valid. Figure 4.7 shows the residual heating oil concentrations for the evaporation loss experiments conducted under enclosed conditions. The difference between the two sets of experiments was that in the first set of experiments the container with the heating oil and water mixture was exposed to the environment while in the second set the container was sealed. The results obtained show that the

heating oil concentration in the solution did not reduce beyond 10 % with a minimum concentration obtained at the 70-min mark of 183 mg/L, which indicated that the experimental setup used for the experiments was valid, and no extensive amounts of heating oil was lost to the environment during the experimental process.

4.6 Sorption of heating oil using blank alginate beads

Once the control for evaporation loss of heating oil was established, it was next necessary to establish a control to determine the amount of oil being sorbed by the alginate beads as it would affect the final reading. This was evaluated by inserting blank alginate beads into the heating oil solution and analyzing the residual oil samples at the respective time steps. Figure 4.8 shows the concentration of the residual oil at the intervals of 10 min, 20 min, 35 min, 70 min, 4 hours and 8 hours.

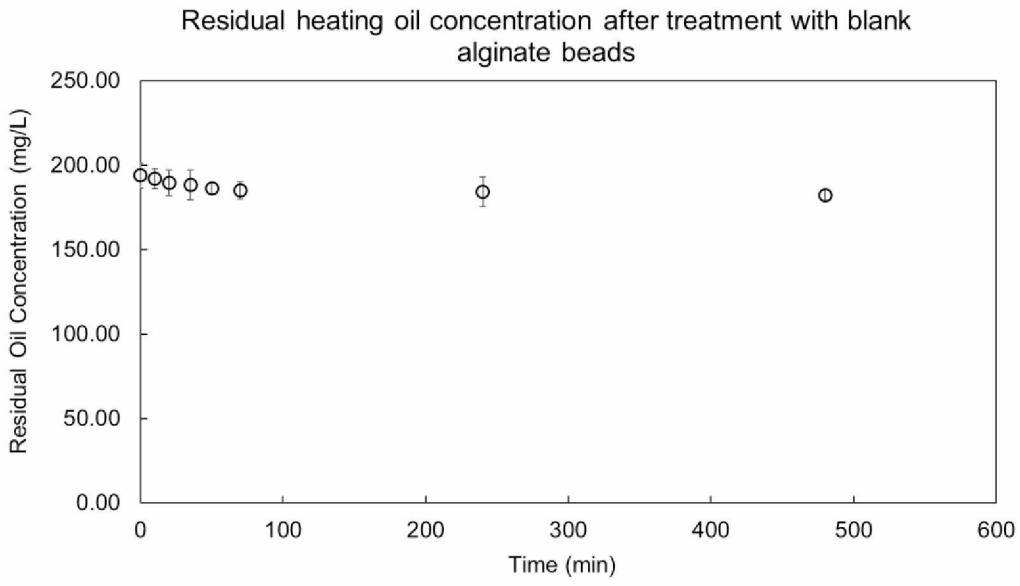

Figure 4.8 Residual heating oil concentration after it was treated with blank alginate beads over a period of 8 hours

It can be observed from the Figure 4.8 that in the initial 10 min the blank alginate beads were able to reduce the concentration of heating oil from 200 mg/L to 190 mg/L. The concentration of heating oil reduced to a minimum of 182 mg/L at the 8-hour mark. This data proved that the alginate beads themselves were unable to remove more than 10 % and established that sorbent needed to be used in order to remove the heating oil from the oil-water mixture.

4.7 Sorption of heating oil using powdered orange peels

Once the effectiveness of orange peels as sorption media was established, we moved on to testing their sorption capacity for heating oil. Two concentrations of powdered orange peels at 4 g/L and 5 g/L were used to study the effect of concentration of orange peels on the sorption of oil. Figure 4.9 shows residual oil concentrations when the orange peel concentration was kept at 4 g/L of water and Figure 4.10 shows the residual oil concentrations when the orange peel concentration is kept at 5 g/L. Analyzing the plots shows that the concentration of heating oil reduces with time. However, from an initial concentration of 200 mg/L, the orange peels are able to remove only about 20% of the heating oil. This shows that the orange peels are not a viable option for use as sorbents of heating oil.

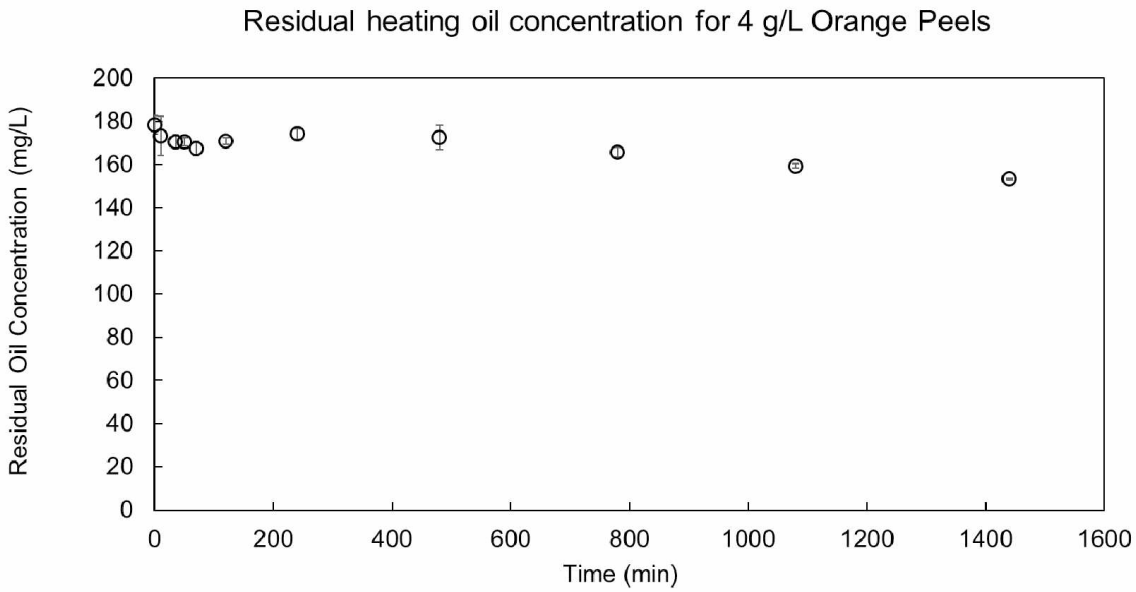

Figure 4.9 Concentration of heating oil remaining in the sample with respect to time after treatment with 4 g/L powdered orange peels

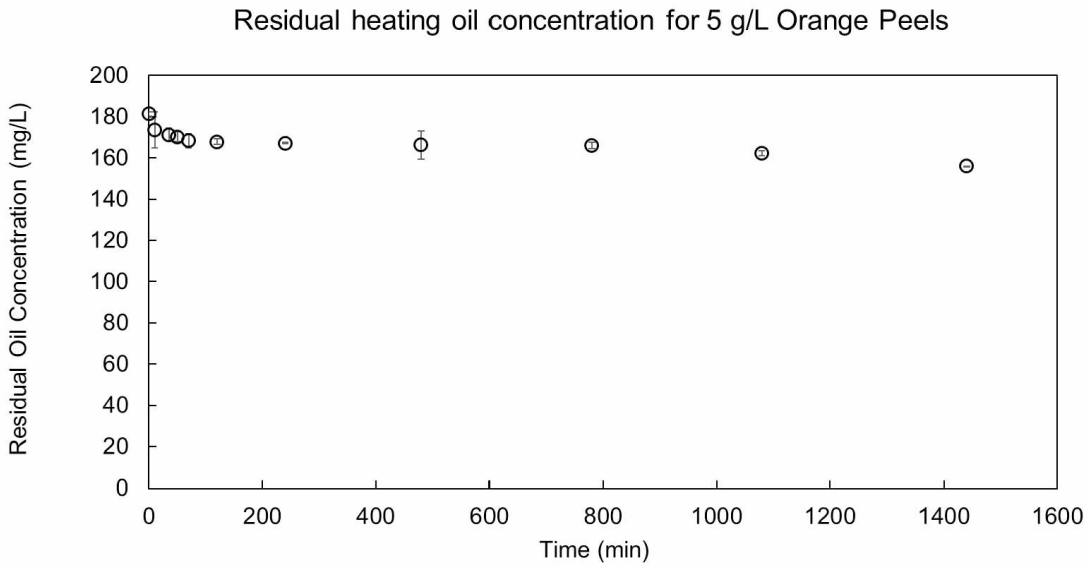

Figure 4.10 Concentration of heating oil remaining in the sample with respect to time after treatment with 5 g/L powdered orange peels

4.8 Sorption of heating oil using alginate encapsulated iron oxide nanoparticles

After the preliminary experiments were carried out using orange peels for sorption of methylene blue and heating oil no. 2, the next stage of the experiments was to evaluate the efficiency of iron oxide nanoparticles, encapsulated in alginate beads, as a medium of sorption. The experiments were carried out as mentioned in chapter 3 with an increasing quantity of iron oxide nanoparticle, from 1g to 5g respectively, being injected into the solution. The residual oil was analyzed using Gas Chromatography & Mass Spectroscopy (GC/MS) instrument. The residual oil concentrations were plotted against time intervals of 10 min, 20 min, 35 min, 50 min, 70 min, 4 hours and 8 hours. Figure 4.11 shows the residual concentration of heating after its treatment with 1g/L of iron oxide nanoparticles encapsulated in alginates beads over a period of 8 hours.

4.8.1 Sorption of heating oil using 1 g/L of iron oxide nanoparticles

It can be observed from Figure 4.11 Concentration of residual heating oil after it was treated with 1 g/L of iron oxide nanoparticles encapsulated in alginate beads over a period of 8 hours that the concentration of the heating oil in the solution reduced from an initial concentration of 200 mg/L to 46 mg/L in the first 10 minutes. At the 20-min mark, the concentration of heating oil present in the solution seems to increase which could be attributed to over saturation of the alginate beads which results in the oil sorbed by the beads to be released back into the solution. This trend seems to continue until the 35-min mark after which the residual oil concentration seems to reach a plateau region of 50 mg/L; at this point, the beads are not able to remove any additional quantity of oil from the solution.

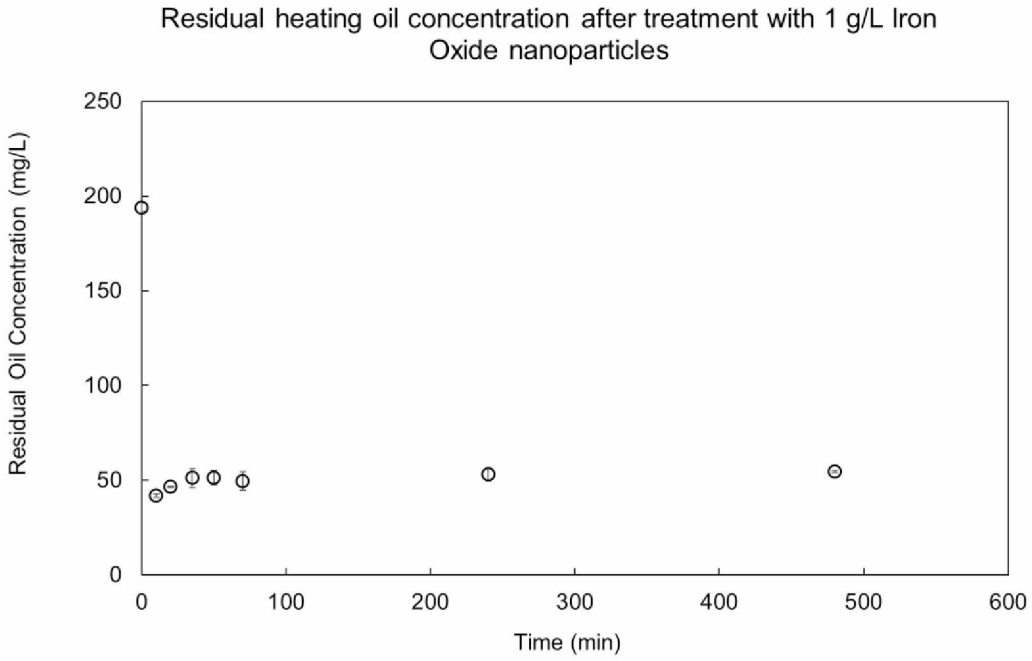

Figure 4.11 Concentration of residual heating oil after it was treated with 1 g/L of iron oxide nanoparticles encapsulated in alginate beads over a period of 8 hours

4.8.2 Sorption of heating oil using 2 g/L of iron oxide nanoparticles

It can be observed from Figure 4.12 that, after treatment with 2 g/L iron oxide nanoparticles, the concentration of the heating oil in the solution reduced from an initial concentration of 200 mg/L to 52 mg/L in the first 10 minutes. At the 20-min mark, the concentration of heating oil present in the solution reduced to 48 mg/L and remained constant until the next 15 min. At 50 min the concentration seems to increase which could be attributed to over saturation of the alginate beads which results in the oil sorbed by the beads to be released back into the solution. At 70 min the concentration drops again to 48 mg/L after which the beads are not able to remove any additional quantity of oil from the solution. This can be observed from the figure as the concentration seems to remain constant for the remainder of the time.

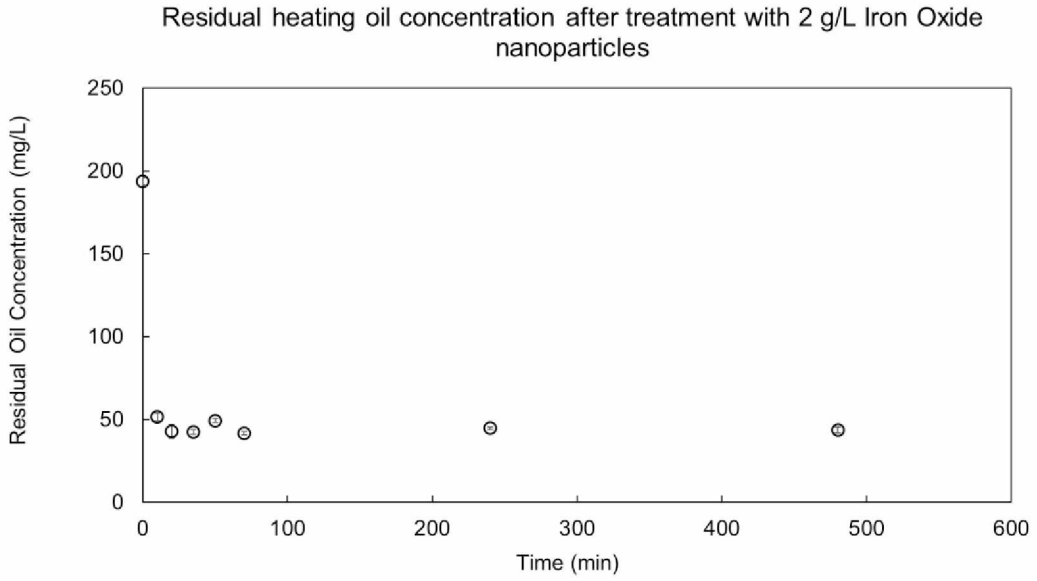

Figure 4.12 Concentration of residual heating oil after it was treated with 2 g/L of iron oxide nanoparticles encapsulated in alginate beads over a period of 8 hours

4.8.3 Sorption of heating oil using 3 g/L of iron oxide nanoparticles

It can be observed from Figure 4.13 that, after treatment with 3 g/L iron oxide nanoparticles, the concentration of the heating oil in the solution reduced from an initial concentration of 200 mg/L to only 100 mg/L in the first 10 minutes. At the 20-min mark, the concentration of heating oil present in the solution seems to reduce to approximately 82 mg/L ± 10. In the next 15 min, the concentration hovers around 90 mg/L and then drops to 50 mg/L after 50 min since the beginning. The concentration thereafter remains constant for the rest of the experiment at a value of 52 mg/L ± 5, the increase in concentration being due to oversaturation of the beads leading to secretion of heating oil back into the solution.

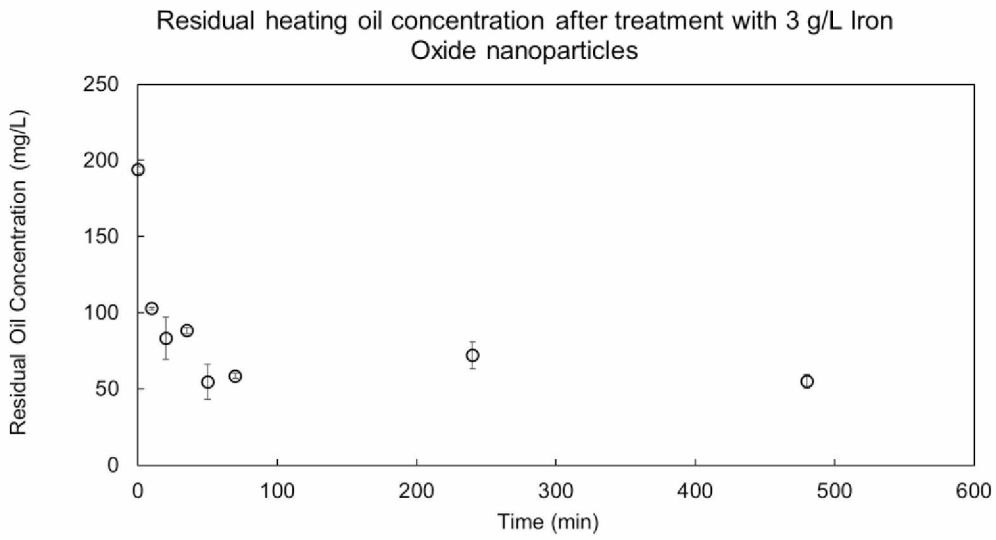

Figure 4.13 Concentration of residual heating oil after it was treated with 3 g/L of iron oxide nanoparticles encapsulated in alginate beads over a period of 8 hours

4.8.4 Sorption of heating oil using 4 g/L of iron oxide nanoparticles

It can be observed from Figure 4.14 that, after treatment with 4 g/L iron oxide nanoparticles, the concentration of the heating oil in the solution reduced from an initial concentration of 200 mg/L to 46 mg/L in the first 10 minutes. At the 20-min mark, the concentration of heating oil present in the solution seems to increase which could be attributed to over saturation of the alginate beads, resulting in the oil sorbed by the beads to be released back into the solution. This trend seems to continue until 35 min after which the residual oil concentration seems to reach a plateau region of 50 mg/L; at this point the beads are not able to remove any additional quantity of oil from the solution.

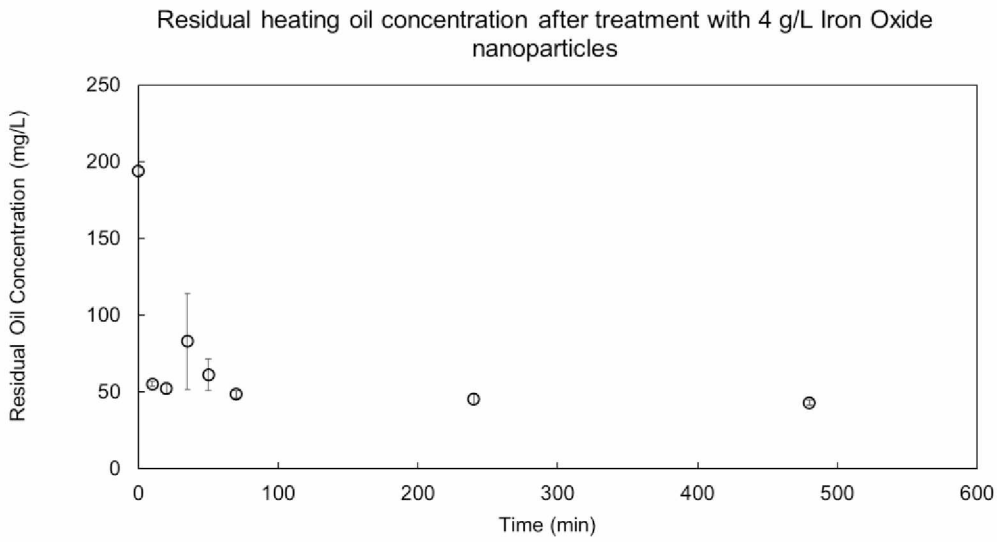

Figure 4.14 Concentration of residual heating oil after it was treated with 4 g/L of iron oxide nanoparticles encapsulated in alginate beads over a period of 8 hours

4.8.5 Sorption of heating oil using 5 g/L of iron oxide nanoparticles

It can be observed from Figure 4.15 that, after treatment with 5 g/L iron oxide nanoparticles, the concentration of the heating oil in the solution reduced from an initial concentration of 200 mg/L to 54 mg/L in the first 10 minutes. At the 20-min mark, the concentration of heating oil present in the solution reduces to approximately 53 mg/L ± 4. In the next 15 min, the concentration of the heating oil seems to increase to 75 mg/L ± 5 which could be attributed to over saturation of the alginate beads which results in the oil sorbed by the beads to be released back into the solution. The concentration thereafter shows a decreasing trend as the residual oil concentration at 50 min is approximately 65 mg/L and it reduces further to 60 mg/L at 70 min and reaches the minimum value of 50 mg/L at 4 hours. The reduction in the concentration of heating oil after 35 min could be attributed to the evaporative loss of the lighter components.

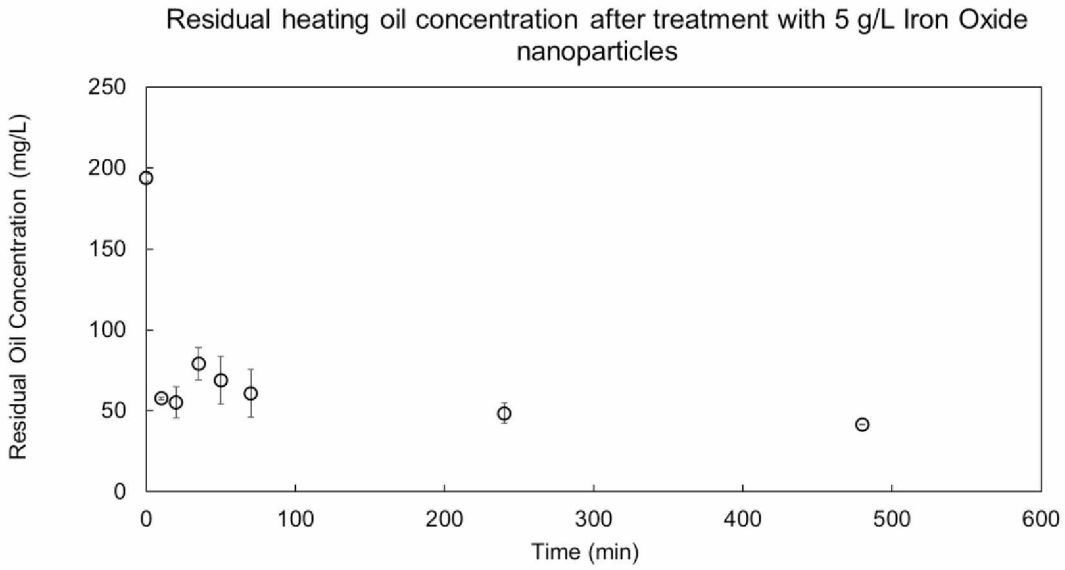

Figure 4.15 Concentration of residual heating oil after it was treated with 5 g/L of iron oxide nanoparticles encapsulated in alginate beads over a period of 8 hours

4.8.6 Selecting the most optimal Iron Oxide nanoparticle concentration for removal of heating oil

Once the experiments involving iron oxide nanoparticles were conducted, the optimal concentration of nanoparticles needed to be determined. Figure 4.16 shows the performance of the five concentrations of iron oxide nanoparticles over a period of eight hours. After comparing the residual oil concentrations of heating oil in the five samples, it was observed that the 2 g of NPs per liter of heating oil and water mixture produced the most optimal results. The concentration of heating oil in the solution went from 200 mg/L to 50 mg/L in the first 10 min and reached a minimum value of 46 mg/L in 20 min which remained constant throughout the duration of the experiment. Compared to the other iron oxide nanoparticle concentrations the 2 g was able to achieve a steady and immediate removal of the heating oil while maintaining the concentration at the same level as opposed to other concentrations where the heating oil secreted back into the solution. Hence, it was decided that the 2 g/L concentration of Iron Oxide nanoparticles was the optimal concentration for the removal of heating oil from the oil and water mixture.

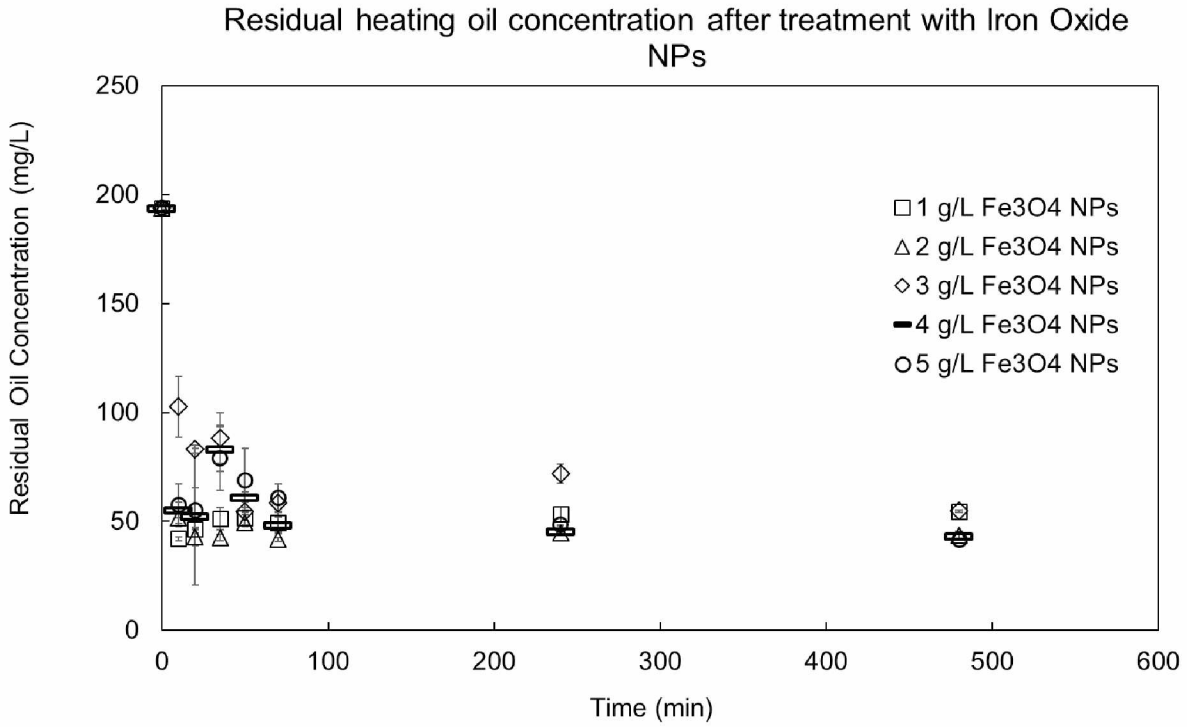

Figure 4.16 Concentration of residual heating oil after it was treated with 5 concentrations of iron oxide nanoparticles encapsulated in alginate beads over a period of 8 hours

4.9 Sorption of heating oil using alginate encapsulated graphene oxide nanoparticles

After the experiments were carried out using iron oxide nanoparticles for sorption of heating oil no. 2, the next step was to evaluate what effect changing the nanoparticle had on the sorption efficiency under the same experimental conditions. For this purpose, graphene oxide nanoparticles were chosen as the medium of sorption Experiments were carried out as mentioned in chapter 3 with increasing quantity of graphene oxide nanoparticle, from 1 g to 3 g respectively, being introduced into the solution. The residual oil was analyzed using Gas Chromatography & Mass Spectroscopy (GC/MS) instrument. The residual oil concentrations were plotted against time intervals of 10 min, 20 min, 35 min, 50 min, 70 min, 4 hours, and 8 hours. Figure 4.17 shows the

residual concentration of heating oil after its treatment with 1g of graphene oxide nanoparticles encapsulated in alginates beads over a period of 8 hours.

4.9.1 Sorption of heating oil using 1 g/L of graphene oxide

It can be observed from Figure 4.17 that, after treatment with 1 g/L graphene oxide nanoparticles, the concentration of the heating oil in the solution reduced from an initial concentration of 200 mg/L to 120 mg/L in the first 10 minutes. At the 20-min mark, the concentration of heating oil present in the solution reduced to 98 mg/L. The concentration of heating oil keeps reducing until 50 min with a low value of 78 mg/L after which the concentration rises to around 100 mg/L. This could be attributed to oversaturation of the nanoparticles leading to a discharge of heating oil back into the solution. The concentration drops again to 75 mg/L at the 4-hour mark as evaporation losses take place and remain constant for the rest of the time.

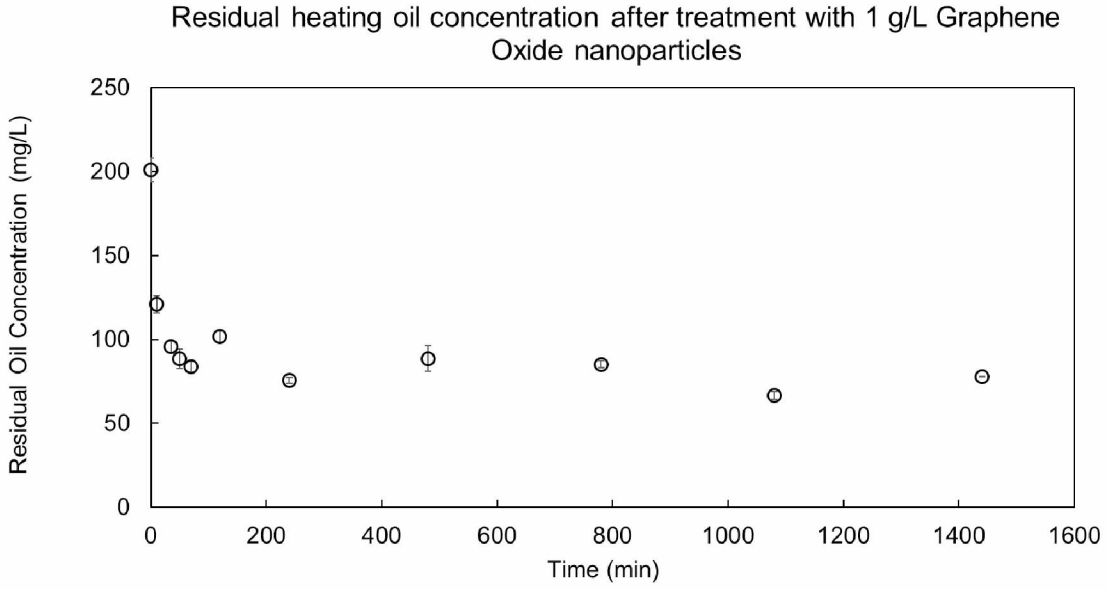

Figure 4.17 Concentration of residual heating oil after it was treated with 1 g/L of graphene oxide nanoparticles encapsulated in alginate beads over a period of 24 hours

4.9.2 Sorption of heating oil using 2 g/L of graphene oxide

It can be observed from Figure 4.18 that, after treatment with 2 g/L graphene oxide nanoparticles, the concentration of the heating oil in the solution reduced from an initial concentration of 200 mg/L to 48 mg/L in the first 10 minutes. In the next 10 min, the concentration reduces to 46 mg/L. This trend continues as the concentration keeps on reducing to reach a minimum of 41 mg/L at the 4-hour mark.

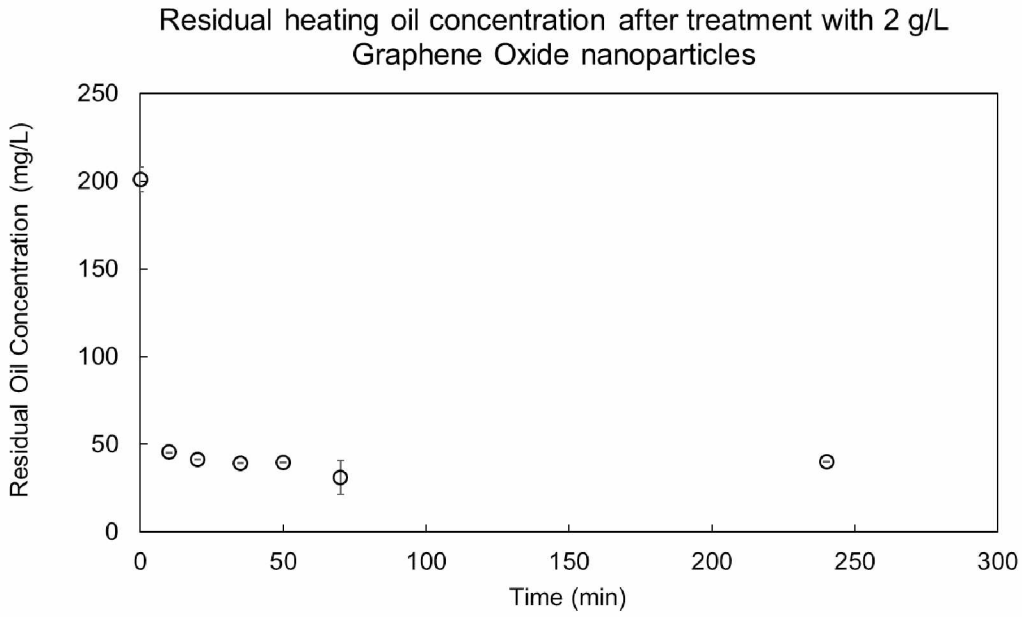

Figure 4.18 Concentration of residual heating oil after it was treated with 2 g/L of graphene oxide nanoparticles encapsulated in alginate beads over a period of 8 hours

4.9.3 Sorption of heating oil using 3 g/L of graphene oxide

It can be observed from Figure 4.19 that, after treatment with 3 g/L graphene oxide nanoparticles, the concentration of the heating oil in the solution reduced from an initial concentration of 200 mg/L to 48 mg/L in the first 10 minutes. At the 35-min mark, the concentration of heating oil present in the solution seems to increase to 64 mg/L which could be attributed to over saturation of the alginate beads which results in the oil sorbed by the beads to be released back into the solution. This trend seems to continue until 75 min, after which the residual

oil concentration reduces back to 52 mg/L which could be explained by the loss of lighter components in the heating oil due to evaporation. The concentration reaches a minimum of 47 mg/L at the 4-hour mark.

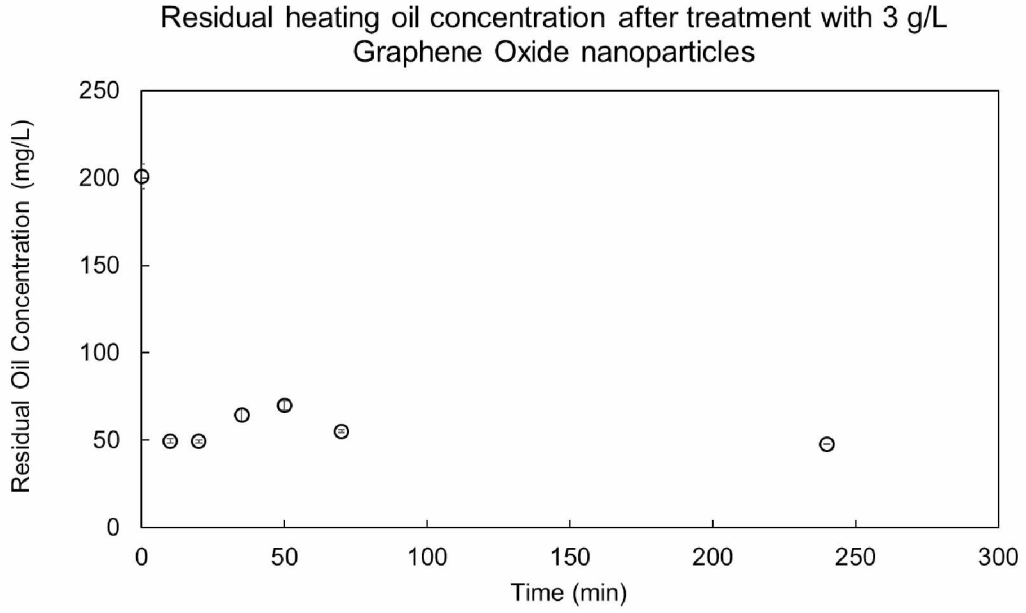

Figure 4.19 Concentration of residual heating oil after it was treated with 3 g/L of graphene oxide nanoparticles encapsulated in alginate beads over a period of 8 hours

4.9.4 Selecting the most optimal Graphene Oxide nanoparticle concentration for removal of heating oil

Once the experiments involving graphene oxide nanoparticles were conducted, the optimal concentration of nanoparticles needed to be determined. Figure 4.20 shows the performance of the five concentrations of iron oxide nanoparticles over a period of eight hours. After comparing the residual oil concentrations of heating oil in the five samples, it was observed that the 2 g of NPs per liter of heating oil and water mixture produced the most optimal results. The concentration of heating oil in the solution went from 200 mg/L to 49 mg/L in the first 10 min and reached a minimum value of 47 mg/L over a period of 70 min which remained constant throughout the duration of the experiment. Compared to the other graphene oxide nanoparticle concentrations, the

2 g was able to achieve a steady and immediate removal of the heating oil while maintaining the concentration at the same level as opposed to other concentrations where the heating oil secreted back into the solution. Hence, it was decided that the 2 g/L concentration of graphene oxide nanoparticles was the optimal concentration for the removal of heating oil from the oil and water mixture.

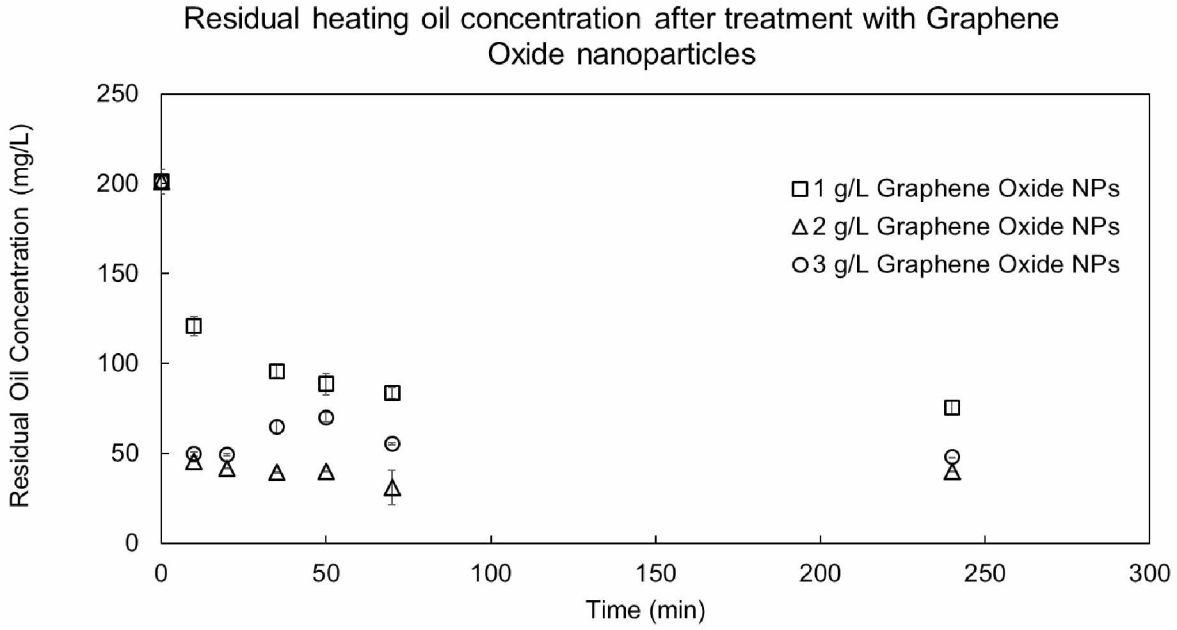

Figure 4.20 Concentration of residual heating oil after it was treated with 5 concentrations of iron oxide nanoparticles encapsulated in alginate beads over a period of 8 hours

4.10 Selecting the optimal sorbent for oil removal

After comparing the results obtained from experimental runs using powdered orange peels, iron oxide nanoparticles, and graphene oxide nanoparticles, it was observed that both iron oxide nanoparticles and graphene oxide nanoparticles were able to remove 75% of the heating oil from the solution in under 10 minutes, and graphene oxide nanoparticles were able to achieve highest oil removal at 81 %, whereas the iron oxide nanoparticles were able to achieve a maximum removal of 77%. As could be observed, there was no significant difference between the efficiency

of the two nanoparticles in the removal of heating oil. The deciding factor in choosing between the two nanoparticles was the cost-effectiveness of the method. Iron oxide nanoparticles (Sigma-Aldrich Product Number - GF18149238) were significantly cheaper in comparison to the graphene oxide nanoparticles (Sigma-Aldrich Product Number – 795534), making the iron oxide nanoparticles the most effective choice.

4.11 Sorption Mechanism of Iron Oxide and Graphene Oxide Nanoparticles

It was observed from the results that the iron oxide and graphene oxide nanoparticles demonstrated different levels of sorption for the heating oil. This could be explained by the sorption mechanisms of both the nanoparticles. According to Gu, Schmitt, Chen, Liang, and McCarthy (1994), the ligand exchange mechanism was responsible for the sorption of organic compounds onto the iron oxide nanoparticles. Other reasons reported by the authors were electrostatic interaction, hydrophobic interaction, entropic effect, hydrogen bonding, and cation bridging for the sorption of organic compounds onto the nanoparticles. The graphene oxide nanoparticles show a different mechanism for the sorption of organics. Pei et al. (2013) posit that sorption mechanisms of organic compounds on graphene oxide nanoparticles can be explained by the charge transfer process and π-π interactions. They also explain that graphene oxide showed a higher affinity for metal ions. The surface area of the nanoparticles used in the experiments also played an important role in the sorption process. The iron oxide nanoparticles used in this study had a surface area in the range of 50 – 245 m^2/g, while the surface area of the graphene oxide nanoparticles were manufactured in-house, the specifications for which can be found in the work of T. Chowdhury (Unpublished work).

4.12 Isotherm study of sorption of heating oil

In order to understand how the change in the amount of nanoparticles added to the solution affected the sorption of heating oil, an isotherm study was conducted. From the residual oil concentration plots for the iron oxide nanoparticles, it could be observed that the encapsulated nanoparticles reached equilibrium concentrations at 70 mins after which the concentration of heating oil in the solution remained constant. In order to develop the isotherms, the residual heating oil concentrations for iron oxide nanoparticles and graphene oxide nanoparticles at 70 mins were used. The ratio of heating oil vs. nanoparticle concentration in the solution was plotted against residual heating oil concentration. It was observed that the log of these values, when plotted for iron oxide, could be fitted to a straight line as shown in Figure 4.21. The Freundlich adsorption isotherm best fits the isotherm model. The isotherm constants can be obtained by comparing the equation of the line to the Freundlich isotherm which is expressed by

$$\log (x/m) = \log K + (1/n) \log c$$

where, x = mass of heating oil

m = mass of nanoparticles in the solution

c = equilibrium concentration of heating oil in the solution

K and n are constants

From, the isotherm plot and the Freundlich isotherm equation we get,

$n = 0.199$

$K = 2.74E\text{-}7\ (mg/g)(L/mg)^{1/n}$

The ratio 1/n indicates the measure of adsorption intensity or surface heterogeneity. A value of $n > 1$ indicated that adsorption intensity was in favor over the range of concentrations used while, $n < 1$ indicated that the reaction favored over higher concentrations and less over lower concentrations. For our experiments, the "n" value was less than 1 which was matched by the

results obtained. P. Xu, Zeng, Huang, Lai, et al. (2012) stated that a value of 1/n below one indicated a normal Freundlich isotherm; however, in our experiments, the 1/n value was higher than one indicating a co-operative adsorption.

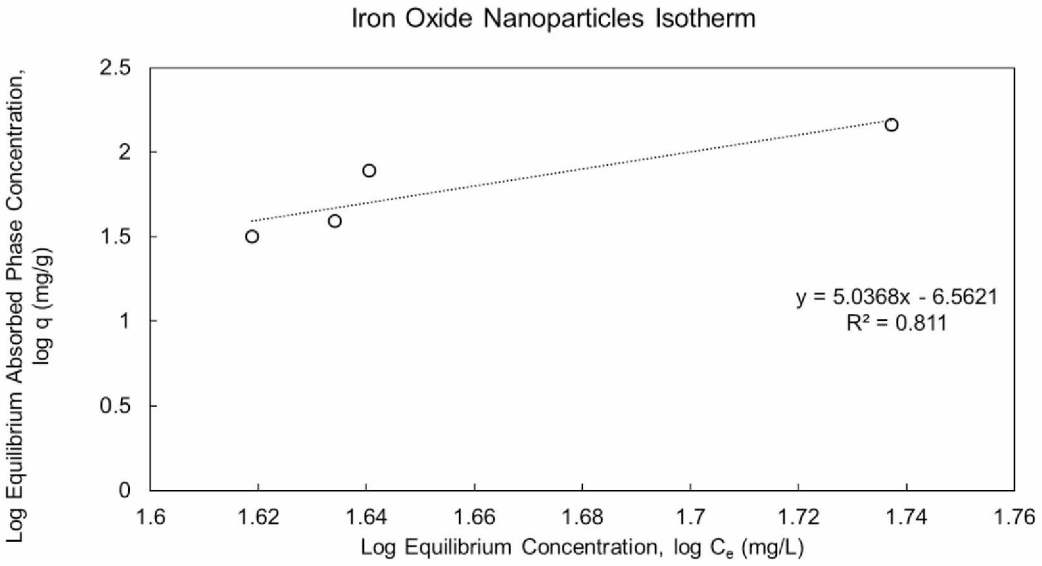

Figure 4.21 Sorption Isotherm developed for iron oxide nanoparticles at the 70 min for nanoparticle concentration of 1 g/L, 2 g/L, 4 g/L, 5 g/L

A similar approach was applied to developing the isotherm of adsorption by graphene oxide nanoparticles. The ratio of residual heating oil concentration vs quantity of graphene oxide nanoparticles in the solution was plotted against the equilibrium concentration of heating oil. The graph obtained was a straight line showing that it is a linear isotherm which is given by,

$q_e = K_{ads} C_e$

solving which we get,

$K_{ads} = 1$ (mg/g) (L/mg)

A linear isotherm is a special case of Freundlich isotherm with 1/n is zero indicating that the reactions were homogenous over the range of concentrations used in the experiments. It indicated that the sorption reaction did not prefer any particular concentration. P. Xu, Zeng, Huang,

Lai, et al., (2012) published the sorption isotherm constants for the adsorption of Pb(II) by iron oxide nanoparticles over a temperature of 298 – 308 K.

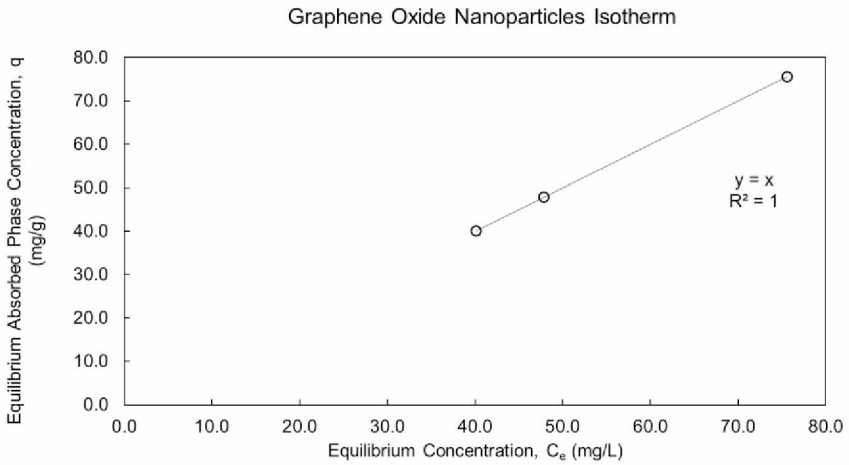

Figure 4.22 Sorption Isotherm developed for graphene oxide nanoparticles at the 70 min for nanoparticle concentration of 1 g/L, 2 g/L, 3 g/L

Table 4.1 Adsorption constants in literature

Sorbent	Contaminant	Isotherm Constant (K, ml/mg)	Source
Iron Oxide NPs	Pb (II)	23.72-33.36	(P. Xu, Zeng, Huang, Lai, et al., 2012)
Iron Oxide NPs	Methylene Blue	10.1	(Mak & Chen, 2004)
Iron Oxide NPs	Dyes	0.89-33.8	(Saha, Das, Saikia, & Das, 2011)
Iron Oxide NPs	Heating oil #2	2.74 E-7	This research
Graphene Oxide NPs	Dye Pollutants	2.89	(H. Sun, Cao, & Lu, 2011)
Graphene Oxide NPs	Co (II)	5.44-6.86	(Liu, Chen, Hu, Wu, & Wang, 2011)
Graphene Oxide NPs	Heating Oil #2	1	This research

4.13 Fluorescence spectroscopy analysis

In order to further establish the effectiveness of nanoparticles in the sorption of heating oil from an oil-water mixture, we conducted fluorescence spectroscopy. Figure 4.23 shows Excitation-Emission Matrix (EEM) for 1 g/L Iron Oxide nanoparticles for a treatment duration of 10 min. An EEM represents the amount of fluorescence a particular component in a sample being analyzed by the fluorescence spectroscope has when bombarded with photons. The higher the fluorescence of the component, the higher the intensity of the peak will be that appears on the EEM.

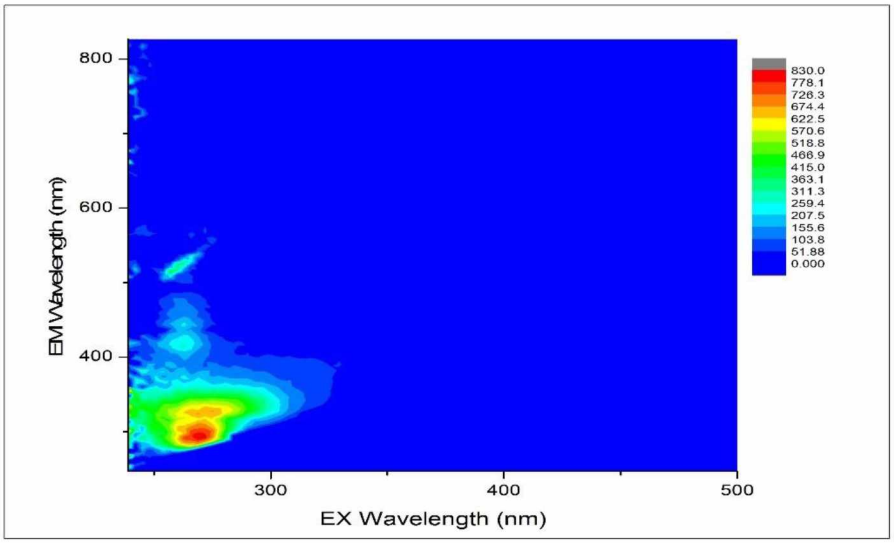

Figure 4.23 Excitation-Emission matrix for 1 g/L Iron Oxide nanoparticles for a treatment duration of 10 min

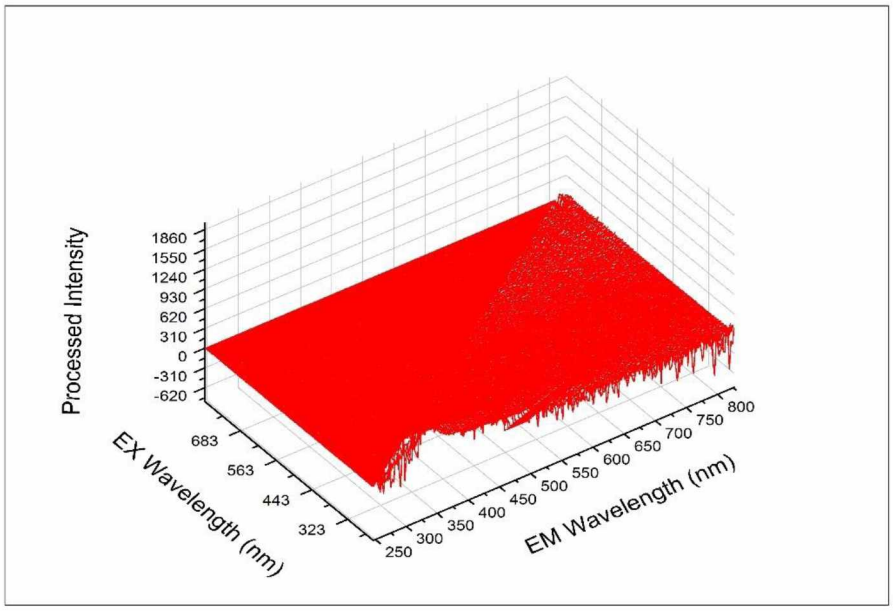

Figure 4.24 3D representation of the Excitation-Emission Matrix for 1 g/L Iron Oxide nanoparticles for a treatment duration of 10 min

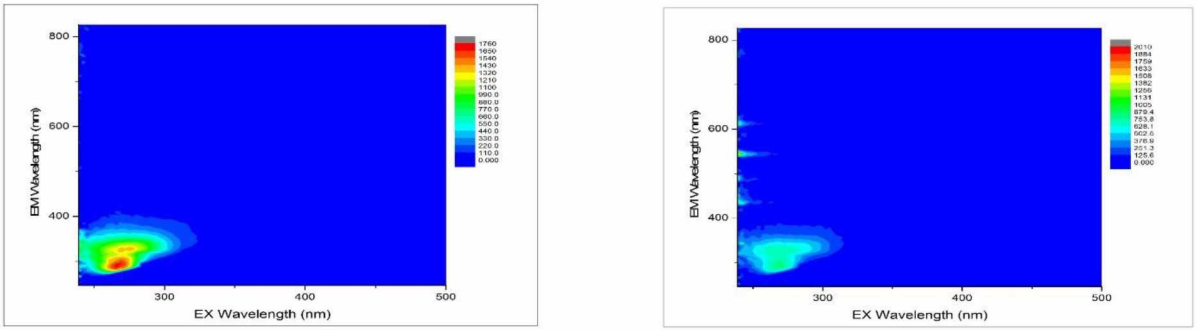

Figure 4.25 Excitation-Emission matrix for 1 g/L Iron Oxide nanoparticles for a treatment duration of 20 min(left) and 70 min(right)

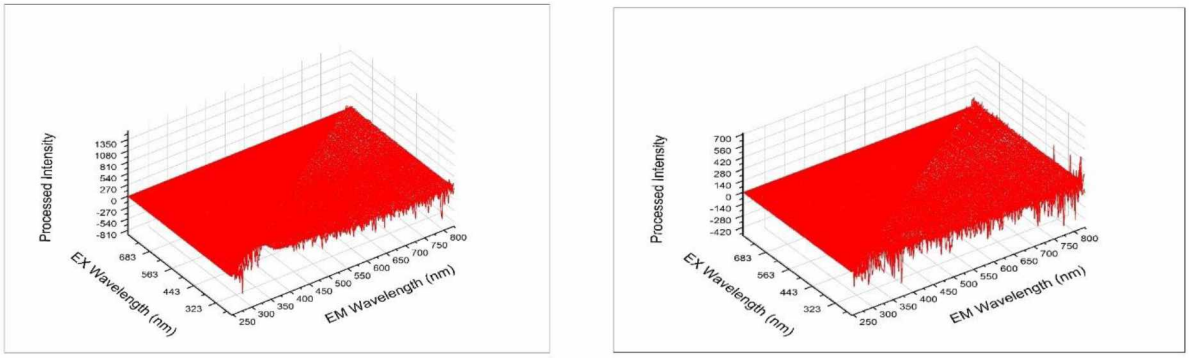

Figure 4.26 3D representation of the Excitation-Emission Matrix for 1 g/L Iron Oxide nanoparticles for a treatment duration of 20 min (left) and 70 min (right)

When the EEMs shown in Figure 4.23 and Figure 4.25 are compared, it becomes evident that the intensity of the fluorescence reduces. This can be directly correlated with the reduction in the quantity of the component of heating oil present in the oil-water solution.

Comparing Figure 4.23, Figure 4.25 indicates that over a period of 70 min the concentration of heating oil reduces in the solution containing an oil-water mixture, which corresponds to the reduction in the intensity of fluorescence in the EEMs. This indicates that iron oxide nanoparticles are able to successfully remove heating oil from the mixture. However, further analysis needs to be carried out in order to establish the efficiency of the process based on fluorescence spectroscopy.

4.14 Comparison with literature

Krajangpan et al. (2008) used calcium alginate bead encapsulated iron nanoparticles for groundwater treatment. They used bare nZVI (nano zerovalent iron) and encapsulated nZVI for the removal of nitrates from the ground water. They studied the removal rate for three concentrations of 100 mg/L, 60 mg/L and 20 mg/L with removal percentage of 73, 62 and 55 respectively for bare nZVI and 73, 57 and 50% for entrapped nZVI over a 2-hour period. Bezbaruah et al. (2011) carried out similar research in which they used calcium alginate

encapsulated iron oxide nanoparticles for the removal of trichloroethylene. They were able to achieve 89-91% removal rate for TCE (trichloroethylene) over a period of 2-hours. Q. Zhu, Tao, and Pan (2010) used hydrophobic Fe_2O_3@C nanoparticles for the removal of lubricating oil from de-ionized water. They were able to adsorb the lubricating oil from the surface water by using the selective adsorbance property of highly hydrophobic nanoparticles; however, no exact measurements have been reported. Moeser, Roach, Green, Laibinis, and Hatton (2002) used magnetized Fe_2O_3 nanoparticles to remove various organics from water. They measured the solubility of various compounds in the presence of the magnetic nanoparticles against the solubility of various compounds in the absence of the nanoparticles to determine the ability of the nanoparticles to remove the organic compounds. The results of their research are summarized in Table 4.2.

Table 4.2 Organic solubility in magnetic fluids and in water

Compound	Solubility in the polymer shell (mol/L)	Solubility in water (mol/L)
Toluene	2.72	5.59 E-3
o-dichlorobenzene	1.75	9.77 E-4
Naphthalene	0.141	2.45 E-4
phenanthrene	0.0677	6.31 E-6
hexane	0.398	1.48 E-4

Karatum et al. (2016) used aerogel composites for the recovery of crude oil and were able to achieve 60-95% for the recovery standards used (2-methylnaphthalene, anthracene, p-terphenyl, benzo[e]pyrene). In our research, we used heating oil number 2 as the contaminant in water and were able to achieve 77% recovery with encapsulated Iron Oxide nanoparticles and 81% recovery

with Graphene Oxide nanoparticles which is comparable to the other established work. The results are summarized in Table 4.3

Table 4.3 Comparison with literature

Nanoparticle/Sorbent	Contaminant	Recovery (%)	Source
nZVI	NO_3-N	55-73	(Krajangpan et al., 2008)
nZVI	TCE	89-91	(Bezbaruah et al., 2011)
Hydrophobic Fe_2O_3	Lubricating Oil	No exact values provided	(Q. Zhu et al., 2010)
Fe_2O_3	Various organics	Provided in **Table 4.2.** Table **4.2**	(Moeser et al., 2002)
Aerogel Composites	Crude Oil	60-95	(Karatum et al., 2016)
Fe_2O_3 Graphene Oxide	Heating Oil No. 2	77 81	This research

Chapter 5 Conclusions and Future Work

In this chapter we will be discussing the conclusions that can be drawn from the results of the experiments conducted to evaluate the efficiency of alginate gel encapsulated powdered orange peels, iron oxide nanoparticles, and graphene oxide nanoparticles in the removal of heating oil number 2 from a mixture of oil and water. We will also suggest what future work needs to be carried out in order to evaluate or establish the effectiveness of the method proposed in this research in order for it to be commercially viable.

5.1 Conclusions

Based on the results obtained from the UV-Vis and GC/MS analysis, it can be concluded that powdered orange peels are not suitable for the removal of heating oil from an oil-water mixture. The orange peels were only able to achieve 20% removal of heating oil from the mixture. Based on the GC/MS data, encapsulated iron oxide nanoparticles were able to achieve a maximum removal of 77% of heating oil from the initial concentration of 200 mg/L in the oil-water mixture. Graphene oxide nanoparticles were able to achieve an approximate removal rate of 81%Both iron oxide nanoparticles and graphene oxide nanoparticles were able to achieve a 75% removal rate for heating oil on average, making them an excellent choice for oil-water separation.

The main factor to consider when making a choice between graphene oxide and iron oxide nanoparticles was the cost difference between the two. Iron oxide nanoparticles (Sigma-Aldrich Product Number GF18149238) were significantly cheaper compared to the graphene oxide nanoparticles (Sigma-Aldrich Product Number – 795534), making the iron oxide nanoparticles the most effective choice. As a result, the final conclusion from this research was that iron oxide nanoparticles were the optimal choice for oil-water separation.

The final conclusions are

1. Encapsulation of nanoparticles in alginate gel does not hinder the efficiency of the nanoparticles to adsorb heating oil.
2. Increasing the duration of contact time between the sorbents and the sorbate increases the removal percentage until 70 min, after which the sorbents reach equilibrium.
3. Graphene oxide nanoparticles perform better than iron oxide nanoparticles; however, the difference is only marginal.

5.2 Future work

1. In the future, we would like to evaluate the reusability of the encapsulated nanoparticles in order to reduce production costs.
2. The effect of coating the nanoparticles with different agents before encapsulation can be evaluated.
3. In our research, we have alginate as the encapsulation medium. Future work could evaluate the effect that the use of different encapsulation materials has on the efficiency of the process
4. The experiments conducted in this research are batch experiments. In the future, we would like to conduct column or continuous experiments.
5. In this research, heating oil was used instead of actual crude oil to facilitate the use of the GC/MS. We would like to test for the efficiency of our process on actual crude oil.
6. Future work could also evaluate the effect of temperature on the efficiency of the process.

References

Afkhami, A., & Moosavi, R. (2010). Adsorptive removal of Congo red, a carcinogenic textile dye, from aqueous solutions by maghemite nanoparticles. *Journal of Hazardous Materials*, *174*(1–3), 398–403. http://doi.org/10.1016/j.jhazmat.2009.09.066

Algothmi, W. M., Bandaru, N. M., Yu, Y., Shapter, J. G., & Ellis, A. V. (2013). Alginate-graphene oxide hybrid gel beads: An efficient copper adsorbent material. *Journal of Colloid and Interface Science*, *397*, 32–38. http://doi.org/10.1016/j.jcis.2013.01.051

Ayati, A., Ahmadpour, A., Bamoharram, F. F., Tanhaei, B., Mänttäri, M., & Sillanpää, M. (2014). A review on catalytic applications of Au/TiO2 nanoparticles in the removal of water pollutant. *Chemosphere*. http://doi.org/10.1016/j.chemosphere.2014.01.040

Bezbaruah, A. N., Shanbhogue, S. S., Simsek, S., & Khan, E. (2011). Encapsulation of iron nanoparticles in alginate biopolymer for trichloroethylene remediation. *Journal of Nanoparticle Research*, *13*(12), 6673–6681. http://doi.org/10.1007/s11051-011-0574-x

Boyer, C., Whittaker, M. R., Bulmus, V., Liu, J., & Davis, T. P. (2010). The design and utility of polymer-stabilized iron-oxide nanoparticles for nanomedicine applications. *NPG Asia Materials*, *2*(1), 23–30. http://doi.org/10.1038/asiamat.2010.6

Broje, V., & Keller, A. A. (2006). Improved mechanical oil spill recovery using an optimized geometry for the skimmer surface. *Environmental Science and Technology*, *40*(24), 7914–7918. http://doi.org/10.1021/es061842m

Cai, X., Tan, S., Yu, A., Zhang, J., Liu, J., Mai, W., & Jiang, Z. (2012). Sodium 1-naphthalenesulfonate-functionalized reduced graphene oxide stabilizes silver nanoparticles with lower cytotoxicity and long-term antibacterial activity. *Chemistry - An Asian Journal*, *7*(7), 1664–1670. http://doi.org/10.1002/asia.201200045

Castro Neto, A. H., Guinea, F., Peres, N. M. R., Novoselov, K. S., & Geim, A. K. (2009). The electronic properties of graphene. *Reviews of Modern Physics*, *81*(1), 109–162. http://doi.org/10.1103/RevModPhys.81.109

Chen, K.-C., & Huang, C.-T. (1988). Effects of the growth of Trichosporon cutaneum in calcium alginate gel beads upon bead structure and oxygen transfer characteristics. *Enzyme and Microbial Technology*, *10*(5), 284–292. http://doi.org/10.1016/0141-0229(88)90129-9

Copland, J. A., Eghtedari, M., Popov, V. L., Kotov, N., Mamedova, N., Motamedi, M., & Oraevsky, A. A. (2004). Bioconjugated gold nanoparticles as a molecular based contrast agent: implications for imaging of deep tumors using optoacoustic tomography. *Molecular Imaging & Biology*, *6*(5), 341–349. http://doi.org/10.1016/j.mibio.2004.06.002

De-Bashan, L. E., Moreno, M., Hernandez, J. P., & Bashan, Y. (2002). Removal of ammonium and phosphorus ions from synthetic wastewater by the microalgae Chlorella vulgaris coimmobilized in alginate beads with the microalgae growth-promoting bacterium Azospirillum brasilense. *Water Research*, *36*(12), 2941–2948. http://doi.org/10.1016/S0043-1354(01)00522-X

Dias, A. M. G. C., Hussain, A., Marcos, A. S., & Roque, A. C. A. (2011). A biotechnological perspective on the application of iron oxide magnetic colloids modified with polysaccharides. *Biotechnology Advances*, *29*(1), 142–155. http://doi.org/10.1016/j.biotechadv.2010.10.003

Feng, L., Cao, M., Ma, X., Zhu, Y., & Hu, C. (2012). Superparamagnetic high-surface-area Fe 3O 4 nanoparticles as adsorbents for arsenic removal. *Journal of Hazardous Materials*, *217–218*, 439–446. http://doi.org/10.1016/j.jhazmat.2012.03.073

Feng, Y., Gong, J.-L., Zeng, G.-M., Niu, Q.-Y., Zhang, H.-Y., Niu, C.-G., … Yan, M. (2010). Adsorption of Cd (II) and Zn (II) from aqueous solutions using magnetic hydroxyapatite nanoparticles as adsorbents. *Chemical Engineering Journal*, *162*(2), 487–494. http://doi.org/10.1016/j.cej.2010.05.049

Fingas, M. (2011). An Overview of In-Situ Burning. In *Oil Spill Science and Technology* (pp. 737–903). http://doi.org/10.1016/B978-1-85617-943-0.10023-1

Giasuddin, A. B. M., Kanel, S. R., & Choi, H. (2007). Adsorption of humic acid onto nanoscale zerovalent iron and its effect on arsenic removal. *Environmental Science & Technology*, *41*(6), 2022–2027. http://doi.org/10.1021/es0616534

Gu, B., Schmitt, J., Chen, Z., Liang, L., & McCarthy, J. F. (1994). Adsorption and desorption of natural organic matter on iron oxide: mechanisms and models. *Environmental Science & Technology*, *28*(1), 38–46. http://doi.org/10.1021/es00050a007

Hamza, L. H., Adly, T. A., & Afifi, S. (2008). Bioremediation - The journey from hazardous to green. *Society of Petroleum Engineers - 9th International Conference on Health, Safety and Environment in Oil and Gas Exploration and Production 2008 - "In Search of Sustainable Excellence," 2*, 769–778. Retrieved from http://www.scopus.com/inward/record.url?eid=2-s2.0-52349098789&partnerID=40&md5=5af9eca753e79db689d13ce2eef28e74

Karatum, O., Steiner, S. A., Griffin, J. S., Shi, W., & Plata, D. L. (2016). Flexible, Mechanically Durable Aerogel Composites for Oil Capture and Recovery. *ACS Applied Materials and Interfaces*, *8*(1), 215–224. http://doi.org/10.1021/acsami.5b08439

Kim, H., Hong, H. J., Jung, J., Kim, S. H., & Yang, J. W. (2010). Degradation of trichloroethylene (TCE) by nanoscale zero-valent iron (nZVI) immobilized in alginate bead. *Journal of Hazardous Materials*, *176*(1–3), 1038–1043. http://doi.org/10.1016/j.jhazmat.2009.11.145

Kistler, S. S. (1932). Coherent Expanded Aerogels. *Rubber Chemistry and Technology*. http://doi.org/10.5254/1.3539386

Krajangpan, S., Jarabek, L., Jepperson, J., Chisholm, B. J., & Bezbaruah, A. (2008). Polymer modified iron nanoparticles for environmental remediation. *235th ACS National Meeting, Abstracts*(February 2015), POLY-520.

Kyzas, G. Z., Deliyanni, E. A., & Matis, K. A. (2014). Graphene oxide and its application as an adsorbent for wastewater treatment. *Journal of Chemical Technology and Biotechnology*. http://doi.org/10.1002/jctb.4220

Lee, Y. C., Kim, C. W., Lee, J. Y., Shin, H. J., & Yang, J. W. (2009). Characterization of nanoscale zero valent iron modified by nonionic surfactant for trichloroethylene removal in the presence of humic acid: A research note. *Desalination and Water Treatment*, *10*(1–3), 33–38. http://doi.org/10.5004/dwt.2009.722

Li, D., Müller, M. B., Gilje, S., Kaner, R. B., & Wallace, G. G. (2008). SI: Processable aqueous dispersions of graphene nanosheets. *Nature Nanotechnology*, *3*(2), 101–5. http://doi.org/10.1038/nnano.2007.451

Li, Q., Mahendra, S., Lyon, D. Y., Brunet, L., Liga, M. V., Li, D., & Alvarez, P. J. J. (2008). Antimicrobial nanomaterials for water disinfection and microbial control: Potential applications and implications. *Water Research*. http://doi.org/10.1016/j.watres.2008.08.015

Liddell, B. V, & Ramert, P. C. (1994). Arctic Bioremediation-A Case Study, (May), 132–136.

Liu, M., Chen, C., Hu, J., Wu, X., & Wang, X. (2011). Synthesis of magnetite/graphene oxide composite and application for cobalt(II) removal. *Journal of Physical Chemistry C*, *115*(51), 25234–25240. http://doi.org/10.1021/jp208575m

Mak, S.-Y., & Chen, D.-H. (2004). Fast adsorption of methylene blue on polyacrylic acid-bound iron oxide magnetic nanoparticles. *Dyes and Pigments*, *61*(1), 93–98. http://doi.org/10.1016/j.dyepig.2003.10.008

McHenry, M. E., & Laughlin, D. E. (2000). Nano-scale materials development for future magnetic applications. *Acta Materialia*, *48*(1), 223–238. http://doi.org/10.1016/S1359-6454(99)00296-7

Mirshahghassemi, S., & Lead, J. R. (2015). Oil Recovery from Water under Environmentally Relevant Conditions Using Magnetic Nanoparticles. *Environmental Science & Technology*, *49*(19), 11729–11736. http://doi.org/10.1021/acs.est.5b02687

Moeser, G. D., Roach, K. A., Green, W. H., Laibinis, P. E., & Hatton, T. A. (2002). Water-Based Magnetic Fluids as Extractants for Synthetic Organic Compounds. *Industrial & Engineering Chemistry Research*, *41*(19), 4739–4749. http://doi.org/10.1021/ie0202118

Mthombeni, N. H., Mpenyana-Monyatsi, L., Onyango, M. S., & Momba, M. N. B. (2012). Breakthrough analysis for water disinfection using silver nanoparticles coated resin beads in fixed-bed column. *Journal of Hazardous Materials*, *217–218*, 133–140. http://doi.org/10.1016/j.jhazmat.2012.03.004

Mullin, J. V., & Champ, M. A. (2003). Introduction/overview to in situ burning of oil spills. *Spill Science and Technology Bulletin*, *8*(4), 323–330. http://doi.org/10.1016/S1353-2561(03)00076-8

Palchoudhury, S., & Lead, J. R. (2014). A Facile and Cost-E ff ective Method for Separation of Oil − Water Mixtures Using Polymer-Coated Iron Oxide Nanoparticles.

Pan, Y. F., Chiou, C. T., & Lin, T. F. (2010). Adsorption of arsenic(V) by iron-oxide-coated diatomite (IOCD). *Environmental Science and Pollution Research*, *17*(8), 1401–1410. http://doi.org/10.1007/s11356-010-0325-z

Pei, Z., Li, L., Sun, L., Zhang, S., Shan, X. Q., Yang, S., & Wen, B. (2013). Adsorption characteristics of 1,2,4-trichlorobenzene, 2,4,6- trichlorophenol, 2-naphthol and naphthalene on graphene and graphene oxide. *Carbon*, *51*(1), 156–163. http://doi.org/10.1016/j.carbon.2012.08.024

Pilipenko, N., Lerondeau, B., & Vial, E. (2013). SPE 166868 Oil Spill Response in the Arctic a . Inconvenients of the existing oil spill recovery solutions, (October), 15–17.

Prabhu, S., & Poulose, E. K. (2012). Silver nanoparticles: mechanism of antimicrobial action, synthesis, medical applications, and toxicity effects. *International Nano Letters*, *2*(1), 32. http://doi.org/10.1186/2228-5326-2-32

Prince, R. C., Lessard, R. R., & Clark, J. R. (2003). Bioremediation of marine oil spills. *Trends in Biotechnology*, *58*(4), 463–468. http://doi.org/10.2516/ogst:2003029

Quang, D. V., Sarawade, P. B., Jeon, S. J., Kim, S. H., Kim, J. K., Chai, Y. G., & Kim, H. T. (2013). Effective water disinfection using silver nanoparticle containing silica beads. *Applied Surface Science*, *266*, 280–287. http://doi.org/10.1016/j.apsusc.2012.11.168

Quevedo, J. A., Patel, G., & Pfeffer, R. (2009). Removal of oil from water by inverse fluidization of aerogels. *Industrial and Engineering Chemistry Research*, *48*(1), 191–201. http://doi.org/10.1021/ie800022e

Rao, C. N. R., Sood, A. K., Subrahmanyam, K. S., & Govindaraj, A. (2009). Graphene: The new two-dimensional nanomaterial. *Angewandte Chemie - International Edition*. http://doi.org/10.1002/anie.200901678

Reynolds, J. G., Coronado, P. R., & Hrubesh, L. W. (2001). Hydrophobic aerogels for oil-spill clean up - Synthesis and characterization. *Journal of Non-Crystalline Solids*, *292*(1–3), 127–137. http://doi.org/10.1016/S0022-3093(01)00882-1

Rocher, V., Bee, A., Siaugue, J. M., & Cabuil, V. (2010). Dye removal from aqueous solution by magnetic alginate beads crosslinked with epichlorohydrin. *Journal of Hazardous Materials*, *178*(1–3), 434–439. http://doi.org/10.1016/j.jhazmat.2010.01.100

Saha, B., Das, S., Saikia, J., & Das, G. (2011). Preferential and enhanced adsorption of different dyes on iron oxide nanoparticles: A comparative study. *Journal of Physical Chemistry C*, *115*(16), 8024–8033. http://doi.org/10.1021/jp109258f

Salehi, R., Arami, M., Mahmoodi, N. M., Bahrami, H., & Khorramfar, S. (2010). Novel biocompatible composite (Chitosan-zinc oxide nanoparticle): Preparation, characterization and dye adsorption properties. *Colloids and Surfaces B: Biointerfaces*, *80*(1), 86–93. http://doi.org/10.1016/j.colsurfb.2010.05.039

Shipley, H. J., Yean, S., Kan, A. T., & Tomson, M. B. (2009). Adsorption of arsenic to magnetite nanoparticles: Effect of particle concentration, pH, ionic strength, and temperature. *Environmental Toxicology and Chemistry*, *28*(3), 509–515. http://doi.org/10.1897/08-155.1

Smidsrod, O., & Skjakbrk, G. (1990). Alginate as immobilization matrix for cells. *Trends in Biotechnology*, *8*, 71–78. http://doi.org/10.1016/0167-7799(90)90139-O

Spies, R. B., Stegeman, J. J., Hinton, D. E., Woodin, B., Smolowitz, R., Okihiro, M., & Shea, D. (1996). Biomarkers of hydrocarbon exposure and sublethal effects in embiotocid fishes from a natural petroleum seep in the Santa Barbara Channel. *Aquatic Toxicology*, *34*(3), 195–219. http://doi.org/10.1016/0166-445X(95)00039-7

Standeker, S., Novak, Z., & Knez, Z. (2007). Adsorption of toxic organic compounds from water with hydrophobic silica aerogels. *Journal of Colloid and Interface Science*, *310*(2), 362–368. http://doi.org/10.1016/j.jcis.2007.02.021

Sun, H., Cao, L., & Lu, L. (2011). Magnetite/reduced graphene oxide nanocomposites: One step solvothermal synthesis and use as a novel platform for removal of dye pollutants. *Nano Research*, *4*(6), 550–562. http://doi.org/10.1007/s12274-011-0111-3

Sun, L., & Fugetsu, B. (2014). Graphene oxide captured for green use: Influence on the structures of calcium alginate and macroporous alginic beads and their application to aqueous removal of acridine orange. *Chemical Engineering Journal*, *240*, 565–573. http://doi.org/10.1016/j.cej.2013.10.083

Ten Hulscher, T. E. M., & Cornelissen, G. (1996). Effect of temperature on sorption equilibrium and sorption kinetics of organic micropollutants - a review. *Chemosphere*, *32*(4), 609–626. http://doi.org/10.1016/0045-6535(95)00345-2

Torres, E., Mata, Y. N., Blazquezy, M. L., Munoz, J. A., Gonzalez, F., & Ballester, A. (2005). Gold and silver uptake and nanoprecipitation on calcium alginate beads. *Langmuir*, *21*(17), 7951–7958. http://doi.org/10.1021/la046852k

Vanem, E., & Endresen, Ø. (2008). Cost-effectiveness criteria for marine oil spill preventive measures. *Reliability Engineering & System Safety*, *93*(9), 1354–1368. http://doi.org/10.1016/j.ress.2007.07.008

Vanem, E., Endresen, Ø., & Skjong, R. (2008). Cost-effectiveness criteria for marine oil spill preventive measures. *Reliability Engineering and System Safety*, *93*(9), 1354–1368. http://doi.org/10.1016/j.ress.2007.07.008

Xiao, Z., Levy-Nissenbaum, E., Alexis, F., Lupták, A., Teply, B. A., Chan, J. M., … Farokhzad, O. C. (2012). Engineering of targeted nanoparticles for cancer therapy using internalizing aptamers isolated by cell-uptake selection. *ACS Nano*, *6*(1), 696–704. http://doi.org/10.1021/nn204165v

Xu, P., Zeng, G. M., Huang, D. L., Feng, C. L., Hu, S., Zhao, M. H., … Liu, Z. F. (2012). Use of iron oxide nanomaterials in wastewater treatment: A review. *Science of the Total Environment*. http://doi.org/10.1016/j.scitotenv.2012.02.023

Xu, P., Zeng, G. M., Huang, D. L., Lai, C., Zhao, M. H., Wei, Z., … Xie, G. X. (2012). Adsorption of Pb(II) by iron oxide nanoparticles immobilized Phanerochaete chrysosporium: Equilibrium, kinetic, thermodynamic and mechanisms analysis. *Chemical Engineering Journal*, *203*, 423–431. http://doi.org/10.1016/j.cej.2012.07.048

Xu, Y., Sheng, K., Li, C., & Shi, G. (2010). Self-assembled graphene hydrogel via a one-step hydrothermal process. *ACS Nano*, *4*(7), 4324–4330. http://doi.org/10.1021/nn101187z

Zhu, Q., Tao, F., & Pan, Q. (2010). Fast and selective removal of oils from water surface via highly hydrophobic core-shell Fe2O3@C nanoparticles under magnetic field. *ACS Applied Materials and Interfaces*, *2*(11), 3141–3146. http://doi.org/10.1021/am1006194

Zhu, Y., Murali, S., Cai, W., Li, X., Suk, J. W., Potts, J. R., & Ruoff, R. S. (2010). Graphene and graphene oxide: Synthesis, properties, and applications. *Advanced Materials*, *22*(35), 3906–3924. http://doi.org/10.1002/adma.201001068